Progress in Polymer Science 75 (2017) 1–30

Contents lists available at ScienceDirect

Progress in Polymer Science

journal homepage: www.elsevier.com/locate/ppolysci

Theoretical modeling and simulations of self-assembly of copolymers in solution

Qian Zhang, Jiaping Lin*, Liquan Wang, Zhanwen Xu

Shanghai Key Laboratory of Advanced Polymeric Materials, State Key Laboratory of Bioreactor Engineering, Key Laboratory for Ultrafine Materials of Ministry of Education, School of Materials Science and Engineering, East China University of Science and Technology, Shanghai, 200237, China

ARTICLE INFO

Article history:
Available online 3 May 2017

Keywords:
Self-assembly of copolymers in solution
Modeling and simulation
Linear copolymer
Branched copolymer
Polymer mixtures
Nanostructure

ABSTRACT

Self-assembly of copolymers in solution is a promising way to prepare novel materials. An accurate control over the self-assembly of copolymers in solution requires a profound understanding about the related thermodynamic rules and kinetic mechanisms. Theoretical modeling and simulation play an increasingly important role in characterizing the structure details and the formation process of polymer assemblies. In this review, we first introduce theoretical modeling and simulation methods that have been applied to investigate the self-assembly of copolymers in solution, including particle-based methods, field-theoretical methods and hybrid modeling methods Then, the application of these methods for the self-assembly of linear block copolymers in solution is highlighted, including the thermodynamic rules and kinetic mechanisms underlying the formation of self-assembled structures. Furthermore, the simulation works of the self-assembly of branched copolymer systems, including graft copolymers, star-like copolymers, dendritic copolymers and bottle-brush copolymers, are addressed. In addition to the one-component polymer systems, simulation investigations of polymer mixture systems are discussed, both the polymer/polymer systems and polymer/nanoparticle systems are considered. Finally, perspectives on the theoretical modeling and simulation in the field of self-assembly of copolymers in solution are presented in the section of concluding remarks and outlook.

Contents

Abbreviations: ADR, Adriamycin; BD, Brownian dynamics; CG, Coarse-grained; CMC, Critical micelle concentration; CUDA, Compute unified device architecture; DDFT, Dynamic density functional theory; DFT, Density functional theory; DLS, Dynamic light scattering; DMFT, Dynamic mean field theory; DPD, Dissipative particle dynamics; EPD, External potential dynamics; GPU, Graphics processing unit; GROMACS, Groningen machine for chemical simulations; HOOMD, Highly optimized object-oriented many-particle dynamics; HPF, Hybrid particle-field; HPH, Solvent-(phobic-philic-phobic) type of triblock copolymer; HS, Hubbard-Stratonovich; LAMMPS, Large-scale atomic/molecular massively parallel simulator; MC, Monte Carlo; MD, Molecular dynamics; MMA, Multimicelle aggregates; MPI, Message passing interface; MV, Multilamellar vesicle; NAMD, Nanoscale molecular dynamics; OpenCL, Open computing language; P2MVP, Poly(2-methylvinylpyridinium iodide); P2VP, Poly(2-vinylpyridine); PAA, Poly(acrylic acid); PAAm, Poly(acryl amide); PB, Polybutadiene; PBLG, Poly(γ-benzyl-L-glutamate); PEE, Polyethylethylene; PEG, Poly(ethylene glycol); PEHA, Poly(2-ethylhexyl acrylate); PEO, Poly(ethylene oxide); PFDA, Poly(1H,1H,2H,2H-perfluorodecyl acrylate); PHH, Solvent-(philic-phobic-phobic) type of triblock copolymer; PHP, Solvent-(philic-phobic-philic) type of triblock copolymer; PLA, Polylactide; PLGA, Poly(L-glutamic acid); POEGA, Poly(oligoethylene glycol acrylate); PPO, Poly(propylene oxide); PS, Polystyrene; PSCF, Polymer self-consistent field; μ-EOF, Poly(ethylethylene-*arm*-ethylene oxide-*arm*-perfluoropropylene oxide); SANS, Small-angle neutron scattering; SAXS, Small-angle X-ray scattering; SCFT, Self-consistent field theory; SMA, Small micelle aggregate; UMA, Unimolecular micelle aggregate.

* Corresponding author.
E-mail address: jlin@ecust.edu.cn (J. Lin).

http://dx.doi.org/10.1016/j.progpolymsci.2017.04.003
0079-6700/

1. Introduction

Self-assembly is a spontaneous organization of components driven by enthalpic and entropic effects [1]. Nature fascinates its self-assembled structures with rich functionality, stimulating scientists from polymer areas to make efforts on self-assembly researches. In bulk, a variety of microstructures, such as lamellae, cylinders, spheres and gyroids, can be formed through the microphase separation between different blocks of copolymers. While in solution, the self-assembly of copolymers involves not only the microphase separation between different blocks but also the macrophase separation between solvents and copolymers. And the incompatibility between solvents and copolymer blocks plays a crucial role in determining the morphology and the formation pathway of the self-assembled structures. Various microstructures such as micelles and vesicles can be obtained by the self-assembly of copolymers in solution [2,3], that provides advanced strategies to mimic the self-assembly processes happened in organisms and prepare functional materials. For example, the micelles self-assembled from poly(ethylene glycol)-*b*-poly(aspartate-hydrazone-adriamycin) (PEG-*b*-p(Asp-Hyd-ADR)) are used to deliver the anticancer drug ADR [4], and the vesicles formed from poly(styrene-*b*-acrylic acid) (PS-*b*-PAA) are suggested as organelle-like nanoreactor for bovine pancreas trypsin [5]. Benefiting from the development of the synthetic chemistry of macromolecules, great progress has been made in this field over past decades. However, the rapid development of synthetic chemistry also brings a larger space for polymer design, and the search of the preparation condition for desired self-assembled structures is more empirical than before. To prepare advanced materials through "bottom-up" approaches and explain the self-assembly processes happened in organisms, an in-depth understanding of the principles underlying the self-assembly of copolymers in solution is necessary.

The self-assembly of copolymers in solution is influenced by a large quantity of controlling factors, such as the rigidity of blocks, the selectivity of solvents for different blocks and the molecular architecture of copolymers, etc. From the viewpoint of experimentalists, it is still a challenge to gain insights into the formation principles of the self-assembled structures. Therefore, the precise preparation and rigorous control of the desired self-assembled structures is still beyond our ability. The theoretical modeling and simulation techniques have already proven to be powerful in studying the thermodynamics and kinetics of the self-assembly of copolymers in bulk [6]. Compared with copolymers in bulk, the self-assembly of copolymers in solution is complicated due to the addition of solvents, that makes the modeling of simulations more challenging. As an example, for the simulation of triblock copolymers, three additional interaction parameters need to be considered if the copolymer system is in solution rather than in bulk. Another roadblock to the theoretical simulation of copolymers in solution is the computing resource. For copolymers in bulk, it is efficient to perform the simulations in cells containing microstructures with one or two periodicities. However, for copolymer solutions, the simulation box should be sufficient large to simulate the equilibrium assemblies and ensure the dilute condition. Fortunately, the development of simulation methods, especially the mesoscopic methods, and the upgrade of computer hardware have enabled us to simulate the self-assembly of copolymer solutions. From these aspects, the theoretical modeling and simulation can provide effective approaches to understand the influences of individual factors on the self-assembly of copolymers in solution and distinguish the thermodynamic stable and metastable structures [7]. The aim of this review is to summarize the recent progress in theoretical simulations regarding the self-assembly of copolymers in solution and then provide a guidance for the experiments in this field.

The present review is organized as follows: In Section 2, the theoretical simulation methods used for investigating the self-assembly of copolymer solutions, including particle-based methods, field-theoretic methods and hybrid modeling methods, are introduced. In this section, we do not propose to offer the detailed description of these simulation methods, but to provide the basic principles, advantages and limitations of them. In Sections 3 and 4, the simulation investigations about the self-assembly behaviors of linear block copolymers and graft copolymers in solution are reviewed, respectively. Both the thermodynamics and the formation kinetics of the self-assembled structures are discussed. In Section 5, the simulation studies about the self-assembly of copolymers with complex architectures including the star-

Table 1
Some software packages available for the theoretical modeling and simulation methods referred in this review. The characteristics of these packages including operating systems, programming language and parallel computing ability are annotated as superscripts.

Simulation methods	Software packages
Molecular dynamics (MD)	GROMACS^{UWCGM}, HOOMD^{UWPGM}, LAMMPS^{UWCGM} and NAMD^{UWCG}
Brownian dynamics (BD)	BDpack^{UFM}, Browndye^{UC}, HOOMD^{UWPGM} and LAMMPS^{UWCGM}
Dissipative particle dynamics (DPD)	DPDmacs^{UC}, HOOMD^{UWPGM} and LAMMPS^{UWCGM}
Monte Carlo (MC)	HOOMD^{UWPGM}, LAMMPS^{UWCGM} and Towhee^{UF}
Field-theoretic polymer simulation (FTPS)	
Self-consistent field theory (SCFT)	PSCF^{UF}
Dynamic mean-field theory (DMFT)	Mesodyn^{WM} (commercial)

^{U} and ^{W} represent that the software package can be executed in Unix-like and Windows operating systems, respectively; ^{C,F} and ^{P} indicate that the package is written in the C language, the FORTRAN and the Python, respectively; ^{M} suggests that the package supports simulations of multiple processors using MPI, and ^{G} implies that the package provides accelerated performance on GPUs.

shaped copolymers, the dendritic copolymers and the bottle-brush copolymers are covered. The difference between these copolymers and linear copolymers or graft copolymers is featured. In Section 6, an overview about the self-assembly of mixture systems in solution is introduced, both the polymer/polymer systems and polymer/nanoparticle systems are discussed. Finally, an outlook of the possible future directions in this field is given.

2. Theoretical modeling and simulation techniques

2.1. Particle-based methods

In this subsection, an overview about the particle-based simulation methods based on atomistic or coarse-grained segment configurations is presented. In the past decades, a variety of particle-based methods have been developed and play an increasingly important role in the fields of computing science. The particle-based methods with different degrees of coarse graining can be used to study systems with different time and length scales. Here, the particle-based methods including molecular dynamics (MD), Brownian dynamics (BD), dissipative particle dynamics (DPD) and Monte Carlo (MC) are featured, and some software packages available for each method are listed in Table 1.

2.1.1. Molecular dynamics

MD is a powerful and versatile simulation technique allowing one to predict the equilibrium and transport properties of a classical many-body system [8–10]. As presented in Table 1, a plenty of free and open-source software packages (*e.g.*, GROMACS, HOOMD, LAMMPS and NAMD) can be utilized to implement MD simulations. The MD method adopts a deterministic approach to perform molecular simulations, meaning that the trajectory in the phase space of the system can be calculated out on the basis of a deterministic physical model. To achieve this goal, three constituents are required to be known in MD simulations: (i) the initial position and velocity of all particles in the simulation box; (ii) the interaction potential or force between any two particles; (iii) the equation of motion obeyed by any particle. In MD, the evolution of particle i is described by Newton's equations of motion

$$m_i \frac{d^2 r_i(t)}{dt^2} = \boldsymbol{F}_i(t), \tag{1}$$

where m_i is the mass of particle i, $\boldsymbol{r}_i(t)$ is the position of particle i at time t and $\boldsymbol{F_i}(t)$ is the force acting on particle i calculated as the negative gradient of the interaction potential U.

It order to obtain an effective numerical solution from Eq. (1) it is necessary to select a number of simulation settings including interaction potential, integration algorithm, boundary condition and ensemble. Since the detailed descriptions of these simulation settings may be found in many books and articles [8–12], here we only briefly feature the selection of interaction potential in MD simulations. In conventional all-atom MD simulations, a typical interaction potential U of a system containing n atoms has the following functional form:

$$U = \sum_{bonds} K_b(b - b_{eq})^2 + \sum_{angles} K_\theta(\theta - \theta_{eq})^2 + \sum_{diherals} \frac{K_\phi}{2}[1 + \cos(m\phi - \phi_{eq})] + \sum_{impr} K_\vartheta(\vartheta - \vartheta_{eq})^2 + \sum_{i=1}^{n-1}\sum_{j>i}^{n} \frac{q_i q_j}{4\pi\epsilon r_{ij}} + \sum_{i=1}^{n-1}\sum_{j>i}^{n} 4\varepsilon\left[\left(\frac{\sigma}{r_{ij}}\right)^{12} - \left(\frac{\sigma}{r_{ij}}\right)^{6}\right], \tag{2}$$

where K_b, K_θ, K_ϕ and K_ϑ are the force constants accounting for the flexibility of molecular configuration; b, θ, ϕ and ϑ are the instantaneous values of bond length, bond angle, dihedral angle and improper angle, respectively; b_{eq}, θ_{eq}, ϕ_{eq} and ϑ_{eq} are the equilibrium values of bond length, bond angle, dihedral angle and improper angle, respectively; m is the multiplicity for dihedral angle; ϵ is the dielectric constant; ε is the Lennard-Jones well depth and σ is the distance at the Lennard-Jones minimum; q_i and q_j are the point partial charges of atoms i and j, respectively; r_{ij} is the distance between atoms i and j. The first two terms in Eq. (2) represent the stretching energy of bonds and the bending energy of bond angles, respectively. The cosine function term reflects the torsion energy of dihedral angles. And the harmonic potential related to the "improper" angle is introduced to simulate the out-of-plane motions of atoms. The remaining two terms in Eq. (2) constitute the non-bonded energy, that can be decomposed into the electrostatic energy (the fifth term) and the van der Waals energy (the sixth term).

An interaction potential such as Eq. (2) can offer a full description of the atomistic interactions and has been widely applied to simulate the biomolecules such as proteins [13–16]. With the help of parallel algorithms and multiprocessor computers, the all-atom MD simulations employing an interaction potential like Eq. (2) can be utilized to simulate the systems comprising a million atoms for a time scale of 100 ns [17]. However, the self-assembly of polymer systems typically involves hundreds of millions of atoms and a much longer time scale [18]. A popular way to solve this problem is the construction of coarse-grained (CG) models. Within CG models, an elementary particle represents a segment of a realistic chain instead of a single atom. And the dihedral angle torsion term, that must be taken into account to calculate the molecular configurations in all-atom simulations, is no longer necessary. To construct the CG model of an atomistic system, two steps need to be accomplished: grouping the atoms into CG sites and establishing the interaction potentials between different CG sites. There exist several procedures to build the CG interaction potential, such as the inverse Boltzmann method, the reverse Monte Carlo method and the force-matching method [19–21]. Although it is essential to develop CG models in a systematic manner, there is no unique CG procedure superior to others.

2.1.2. Brownian dynamics

BD is a simple form of stochastic dynamics, in which the evolution of particle i is described by Langevin equation [12,22,23]

$$m_i \frac{d^2 r_i(t)}{dt^2} = \sum_{j \neq i} \boldsymbol{F}_{ij}^{C}(t) - \gamma \boldsymbol{p}_i(t) + \sqrt{2\gamma k_B T}\boldsymbol{\zeta}_i(t), \tag{3}$$

where $\boldsymbol{F}_{ij}^{C}(t)$ is the conservative force exerted by particle j on particle i at time t, $\boldsymbol{p}_i(t)$ is the momentum of particle i, γ is the friction coefficient, k_B is the Boltzmann constant, T is the temperature and $\boldsymbol{\zeta}_i(t)$ is the Gaussian random noise term.

In contrast to the MD method, the BD method adopts an implicit continuum solvent description to enhance the computing efficiency. In BD simulations, the effects of solvents on solute particles are represented through the dissipative and the random force terms. And the internal motions of particles in BD simulations are ignored. These simplifications enable BD to be particularly useful when a system, such as the polymer solutions, exhibits a large gap of time scales governing the time evolution of different components [12,24]. However, instead of fully modeling the implicit solvent condition, only the viscous aspect of solvent molecules is considered in BD method, that restricts its application in many conditions. For example, to simulate the solvent-phobic effect in polymer solutions, the conservative forces acting on solute particles have to be modified [25]. Additionally, the energy and momentum in BD systems are not conserved. In other words, it is unable to consider the hydrodynamic effects correctly through BD technique. Some modified BD methods have been proposed to overcome this problem [26,27]. Although there are ways of considering the hydrodynamic effects in BD simulations, the MD or DPD simulation with explicit solvents should be considered if a precise description of hydrodynamic interaction is required.

2.1.3. Dissipative particle dynamics

DPD, first proposed by Hoogerbrugge and Koelman and reformulated by Groot and co-workers, is a mesoscale computational method that has shown to be powerful in simulating the complex fluid systems [28–31]. A number of free and open-source software packages, such as DPDmacs, HOOMD and LAMMPS, can be utilized to implement DPD simulations. Similar to MD simulations, the solvent molecules are considered explicitly in DPD simulations. However, the elementary particle in DPD simulations is not an atom or molecule but a cluster of molecules. In DPD simulations, the time evolution of the elementary particles is governed by Newton's equations of motion, and the force acting on particle i is a sum of pairwise conservative $\boldsymbol{F}_{ij}^{C}(t)$, dissipative $\boldsymbol{F}_{ij}^{D}(t)$ and random forces $\boldsymbol{F}_{ij}^{R}(t)$ [32,33]

$$\boldsymbol{F}_i(t) = \sum_{j \neq i} (\boldsymbol{F}_{ij}^{C}(t) + \boldsymbol{F}_{ij}^{D}(t) + \boldsymbol{F}_{ij}^{R}(t)), \tag{4}$$

$$\boldsymbol{F}_{ij}^{C}(t) = \begin{cases} a_{ij}(1 - r_{ij}/r_c)\hat{\boldsymbol{r}}_{ij} & (r_{ij} < r_c) \\ 0 & (r_{ij} \geq r_c) \end{cases}, \tag{5}$$

$$\boldsymbol{F}_{ij}^{D}(t) = -\gamma\omega^{D}(\boldsymbol{r}_{ij})(\hat{\boldsymbol{r}}_{ij} \cdot v_{ij})\hat{\boldsymbol{r}}_{ij}, \tag{6}$$

$$\boldsymbol{F}_{ij}^{R}(t) = \sigma\omega^{R}(\boldsymbol{r}_{ij})\theta_{ij}\hat{\boldsymbol{r}}_{ij}, \tag{7}$$

where a_{ij} is the maximum repulsion interaction between particle i and particle j, r_c is the cutoff radius, $\hat{\boldsymbol{r}}_{ij} = \boldsymbol{r}_{ij}/\boldsymbol{r}_{ij}$ is an unit vector, σ is the noise amplitude, θ_{ij} is a randomly noise term with a Gaussian distribution and unit variance, $\omega^{D}(r)$ and $\omega^{R}(r)$ are r-dependent weight functions vanishing for $r \geq r_c$.

In contrast to BD, the pairwise dissipative and random forces in DPD serve as a thermostat together and ensure the conservation of momentum. In other words, the hydrodynamic interactions, that may be important in the self-assembly process of polymers in solution, can be simulated correctly in DPD. Although the atomistic details is lost in DPD method, it possesses several advantages over MD. Primarily, compared with MD simulations, the number of particles required for the investigations of hydrodynamic behaviors in DPD simulations is much smaller. Second, the soft conservative force in DPD decreases linearly with increasing r_{ij}, that allows for larger time steps to be adopted than those in MD. Finally, the relation between the repulsion conservative force of DPD and the χ-parameters in Flory-Huggins theory can be established [31], that effectively bridges the gap between the atomistic simulations and the mesoscopic simulations.

2.1.4. Monte Carlo

Unlike the deterministic MD method, the MC method is a stochastic approach that employs random numbers to generate the sample population of the system and achieve the thermodynamic equilibrium state. Since the detailed descriptions of MC method can be found in other literatures [34,35], here we only give a brief description of the importance sampling MC simulation of a system containing n particles: (i) for the system with initial configuration of $\{\boldsymbol{r}_1, \boldsymbol{r}_2, \cdots, \boldsymbol{r}_n\}$, the energy of the system $U\{\boldsymbol{r}_1, \boldsymbol{r}_2, \cdots, \boldsymbol{r}_n\}$ is calculated; (ii) changing the position of the particle i from $\boldsymbol{r}_i$ to $\boldsymbol{r}_i'$, and calculating the change of the system energy $\Delta U = U\{\boldsymbol{r}_1, \cdots, \boldsymbol{r}_i', \cdots, \boldsymbol{r}_n\} - U\{\boldsymbol{r}_1, \cdots, \boldsymbol{r}_i, \cdots, \boldsymbol{r}_n\}$; (iii) if there exists $\Delta U < 0$, the new position $\boldsymbol{r}_i'$ is accepted, while if there exists $\Delta U \geq 0$, a random number $\eta \in [0,1]$ is generated and the position $\boldsymbol{r}_i'$ can be accepted only if $\exp\left(-\frac{\Delta U}{k_B T}\right) \geq \eta$ is true, and the above steps are repeated until the configuration of the system has been updated completely. In a successful MC simulation, the same equilibrium state should be reached via finite MC steps from any initial state, that always requires two constraints: ergodicity and detailed balance. Ergodicity requires that every configuration with nonzero Boltzmann weight can be accessed by finite MC steps from any initial configuration. And the detailed balance requires that the transition rate of a configuration transition from $\{\boldsymbol{r}_1, \cdots, \boldsymbol{r}_i, \cdots, \boldsymbol{r}_n\}$ to $\{\boldsymbol{r}_1, \cdots, \boldsymbol{r}_i', \cdots, \boldsymbol{r}_n\}$ equals that of the reversed transition from $\{\boldsymbol{r}_1, \cdots, \boldsymbol{r}_i', \cdots, \boldsymbol{r}_n\}$ to $\{\boldsymbol{r}_1, \cdots, \boldsymbol{r}_i, \cdots, \boldsymbol{r}_n\}$.

Both lattice and off-lattice (continuum space) models can be adopted in a MC simulation. Compared with simulations using off-lattice model, the time cost of simulations with lattice model can be drastically reduced [36–39]. Therefore, the lattice model is usually employed to simulate polymer systems in MC simulations. According to the algorithm generating the molecular conformation, the MC methods can be divided into static methods or dynamic methods [40–42]. In static MC methods, there is no relationship between the simulation results of two sequential MC steps. In dynamic MC methods, the sampling technique of molecular conformation is based on a realistic model of the corresponding physical process. In summary, the MC method has two advantages over the MD method: first, the calculations of the forces are avoided in MC simulations; second, the MC simulations can be applied to study the statistical physics in polymer science, beyond the ability of MD method. However, it must be noted that the dynamic process represented by MC method is a mathematic approximation rather than a physical dynamics.

2.2. Field-theoretic methods

Although the above-mentioned particle-based methods have already made some progress in the fields of polymeric self-assembly [6], they have several intrinsic drawbacks. For example, it takes a long time for particle-based methods to equilibrate a polymer system with a large length scale, and computationally expensive techniques, such as the Ewald summation, are required for employing particle-based methods to study the systems with long-ranged interactions [43–45]. The field-theoretic methods have proven to be efficient for studying the equilibrium properties in a number of polymer systems [46,47]. In particular, the field-theoretic methods are rather good at analyzing the thermodynamic stability of self-assembled structures. In the present subsection, the field-theoretic methods including field-theoretic

polymer simulation (FTPS), self-consistent field theory (SCFT) and dynamic mean field theory (DMFT) are introduced, both the advantages and limitations of these methods are discussed.

Before introducing the implementation details of FTPS, SCFT and DMFT, it is helpful to present the unified theoretical framework underlying these field-theoretic methods. Taking AB diblock copolymer as an example, the canonical ensemble partition function of a system containing n_{AB} incompressible AB diblock copolymers with the polymerization index of N and the block composition of f_A in a volume V can be written as

$$Z = \int DW_+ \int DW_- \exp(-H[W_+, W_-]), \tag{8}$$

where W_+ and W_- are the fluctuating chemical potential fields introduced through HS transformation, $\int DW$ is a functional integral over the chemical potential fields, and $H[W_+,W_-]$ is the complex effective Hamiltonian given by (see [47] for a more detailed discussion)

$$H[W_+, W_-] = C\int d\boldsymbol{r}\left(\frac{{W_-}^2(\boldsymbol{r})}{\chi_{AB}N} - iW_+(\boldsymbol{r})\right) - CV\ln Q[iW_+ - W_-, iW_+ + W_-], \tag{9}$$

where $C = n_{AB}{R_g}^3/V$ is the dimensionless chain concentration, R_g is the radius of gyration, χ_{AB} is the Flory-Huggins interaction parameter between the A and B segments, $Q[iW_+-W_-,iW_++W_-]$ is the partition function of a single diblock copolymer chain evaluated through the chain propagator $q(\boldsymbol{r},s)$

$$Q[iW_+ - W_-, iW_+ + W_-] = \frac{1}{V}\int d\boldsymbol{r}q(\boldsymbol{r}, s = 1), \tag{10}$$

where s denotes the chain contour. The chain propagator $q(\boldsymbol{r},s)$ is obtained by solving the modified diffusion equation

$$\frac{\partial}{\partial s}q(\boldsymbol{r}, s) = \nabla^2 q(\boldsymbol{r}, s) - w(\boldsymbol{r}, s)q(\boldsymbol{r}, s), \tag{11}$$

that is subjected to the initial condition of $q(\boldsymbol{r},s{=}0){=}1$ and with $w(\boldsymbol{r},s)$ defined by

$$w(\boldsymbol{r}, s) = \begin{cases} iW_+(\boldsymbol{r}) - W_-(\boldsymbol{r}) & (s \le f_A) \\ iW_+(\boldsymbol{r}) + W_-(\boldsymbol{r}) & (s > f_A) \end{cases}. \tag{12}$$

The Eqs. ((8)–(12)) constitute the field-theoretic model of AB diblock copolymers. It must be mentioned that both the chain propagator $q(\boldsymbol{r},s)$ and the single chain partition function $Q[iW_+,W_-]$ are complex quantities. In the field-theoretic model of AB diblock copolymers, the reduced density operators $\phi_A(\boldsymbol{r};[W_\pm])$ and $\phi_B(\boldsymbol{r};[W_\pm])$ are calculated from the chain propagator $q(\boldsymbol{r},s)$ and the corresponding complementary propagator $q^\dagger(\boldsymbol{r},s)$

$$\phi_A(\boldsymbol{r}; [W_\pm]) = \frac{1}{Q}\int_0^{f_A} dsq(\boldsymbol{r}, s)q^\dagger(\boldsymbol{r}, 1-s), \tag{13}$$

$$\phi_B(\boldsymbol{r}; [W_\pm]) = \frac{1}{Q}\int_{f_A}^{f_A} dsq(\boldsymbol{r}, s)q^\dagger(\boldsymbol{r}, 1-s). \tag{14}$$

In practice, there are several strategies to evaluate the field-theoretic model of polymer systems: (i) generate the numerical approximations to the exact field theory, referred to as the FTPS technique; (ii) impose analytical approximations to simplify the theory and then use analytical or numerical methods to extract information from the simplified theory.

2.2.1. Field-theoretic polymer simulation

A convenient approach to implement FTPS is to employ the complex Langevin technique to sample the chemical potential fields $W_\pm(\boldsymbol{r},t)$

$$\frac{\partial W_{\pm,R}(\boldsymbol{r}, t)}{\partial t} = -\lambda_\pm Re[\frac{\delta H[W_+, W_-]}{\delta W_\pm}] + \eta_\pm(\boldsymbol{r}, t), \tag{15}$$

$$\frac{\partial W_{\pm,I}(\boldsymbol{r}, t)}{\partial t} = -\lambda_\pm Im[\frac{\delta H[W_+, W_-]}{\delta W_\pm}], \tag{16}$$

where subscripts R and I denote the real and imaginary parts of a complex quantity, respectively. t is a fictitious time without physical significance and $\lambda_\pm > 0$ are relaxation rate coefficients, $\eta_\pm(\boldsymbol{r},t)$ are the Gaussian random noise fields that obeys the following statistics

$$\langle(\eta_\pm(\boldsymbol{r}, t))\rangle = 0, \tag{17}$$

$$\langle\eta_\pm(\boldsymbol{r}, t)\eta_\pm\left(\boldsymbol{r}', t'\right)\rangle = 2\lambda_\pm\delta\left(\boldsymbol{r} - \boldsymbol{r}'\right)\delta\left(t - t'\right). \tag{18}$$

In addition to the complex Langevin technique, other numerical methods such as force-bias or hybrid Monte Carlo technique can also be used to implement FTPS, one can find more details of FTPS in Fredrickson's book [47].

2.2.2. Self-consistent field theory

In contrast to FTPS, SCFT method belongs to the second type of strategies for investigating the equilibrium properties of polymer systems. The SCF theory, a mesoscopic polymer theory originally proposed by Edwards in the 1960s [48] and adapted by Helfand to treat block copolymers in the 1970s [49,50], is a type of mean-field theory that can be viewed as a saddle point approximation to the field-theoretic model. In SCFT simulations, the mean-field approximation is invoked so that all configurations can be neglected except for a single "saddle point" configuration. This field configuration is obtained by

$$\frac{\delta H[W_+, W_-]}{\delta W_\pm}|_{W_{\pm*}} = 0, \tag{19}$$

where $W_+{}^*(\boldsymbol{r})$ and $W_-{}^*(\boldsymbol{r})$ are the "mean chemical potential fields" associated with the saddle point configuration. Considering that $H[W_\pm{}^*]$ must be real for any physical saddle point, Eq. (19) can be reduced to

$$Im[\frac{\delta H[W_+, W_-]}{\delta W_+}]_{W_{\pm*}} = 0, \tag{20}$$

$$Re[\frac{\delta H[W_+, W_-]}{\delta W_-}]_{W_{\pm*}} = 0. \tag{21}$$

In general, SCFT simulations can be carried out through spectral methods [51,52] and real space methods [53–56]. Among these numerical techniques, an efficient way developed by Fredrickson et al. [55,56] for computing saddle points is to write non-conserved relaxation scheme of chemical potential fields

$$\frac{\partial W_{+,I}(\boldsymbol{r}, t)}{\partial t} = -\lambda_+ Im[\frac{\delta H[W_+, W_-]}{\delta W_+}], \tag{22}$$

$$\frac{\partial W_{-,R}(\boldsymbol{r}, t)}{\partial t} = -\lambda_- Re[\frac{\delta H[W_+, W_-]}{\delta W_-}]. \tag{23}$$

Compared with FTPS technique, SCFT is more efficient to investigate the thermodynamic properties of polymer systems in which the mean-field approximation is valid. However, it should be noted that the accuracy of the mean-field approaches, such as the SCFT and the DMFT, are affected by the dimensionless chain concentration C. For systems with a low value of C, such as the polymer solutions in dilute or semi-dilute regimes, the functional integral defining the configuration partition function of the field-theoretic

model is not entirely dominated by the "saddle point" configuration and the mean-field methods may lose their accuracy [46]. Under these circumstances, the mean-field calculations are suggested to be initiatory explorations. The technique for direct sampling of field-theoretic models without any approximations, *i.e.*, the FTPS technique, is a promising way to tackle this problem.

2.2.3. Dynamic mean-field theory

The DMFT, sometimes is referred to as dynamic SCFT or dynamic density field theory (DDFT), is a dynamical version of mean-field theory that extends Cahn-Hilliard dynamics to SCF theory [57–59]. This approach consists of two ingredients: the derivation of the chemical potential $\mu(\boldsymbol{r})$ and a diffusion dynamics that relates the chemical potential to the evolution of the density fields $\phi(r)$. In the simplest form of DMFT method, the time evolution equation for the density fields of the K segment $\phi_K(\boldsymbol{r},t)$ is written as

$$\frac{\partial \phi_K(\boldsymbol{r},t)}{\partial t} = M_K \nabla \cdot [\phi_K(\boldsymbol{r},t) \nabla \mu_K(\boldsymbol{r},t)], \tag{24}$$

where M_K is diffusion coefficient that relies on the polymer-specific kinetic factors. The chemical potentials $\mu_K(\boldsymbol{r},t)$ are obtained by applying the local equilibrium condition at each time t

$$\frac{\delta H[\phi,\mu]}{\delta \mu_K(\boldsymbol{r},t)} = 0. \tag{25}$$

By comparison with the experiments conducted under weakly non-equilibrium conditions, the DMFT method defined by Eqs. (24) and (25) proves to be effective to simulate processes with length and time scales presently inaccessible by MD simulations [60]. Additionally, DMFT can be implemented by the software package of Mesodyn from Accelrys [61], that makes DMFT method an easily implemented simulation technique. Nevertheless, it is difficult for the DMFT method to consider the nonlocal coupling effect because the huge computational expense to obtain the chemical potential $\mu(\boldsymbol{r})$ at each time step. To study the nonlocal coupling effect, Maurits and Fraaije developed a feasible method named external potential dynamics (EPD) [62]. In contrast to DMFT, the polymer dynamics is described by the external potential dynamics equations in EPD

$$\frac{\partial W(r,t)}{\partial t} = -M\nabla^2(\mu(\boldsymbol{r}) + \eta(\boldsymbol{r},t)), \tag{26}$$

in which the Rouse-like dynamics can be simulated more efficiently through a local diffusion coefficient. Furthermore, by taking the momentum into consideration, the influence of hydrodynamic force on the self-assembly of polymers in solution can be investigated, a direction for future development in this area.

2.3. Hybrid modeling methods

Both the particle-based methods and the field-theoretic methods have their advantages and limitations. For instance, the field-theoretic methods exhibit high-efficiency in exploring the thermodynamic equilibrium state of polymer systems while the particle-based simulations often need a large number of computational resources, and the particle-based simulations can present the segmental details that may be ignored in field-theoretic methods. In the decades, the hybrid strategy to develop simulation techniques possessing the advantages of existing methods and avoiding their shortages has attracted a lot of attention [63–68]. In the hybrid modeling strategy, the specified part in the system is described by spatial coordinate whereas the rest of the system is represented in terms of density field, and the particle-based and field-theoretic calculations are performed simultaneously and interactively. As an instance, a hybrid method combining DDFT with DPD has been proposed by Kyrylyuk et al. to study the self-assembly of oil/water/surfactant mixtures [67]. In their DDFT/DPD simulations, the surfactants are modeled as short block copolymers on basis of DPD method and the immiscible oil/water mixtures is simulated by SCFT approach. Another example is the hybrid particle-field (HPF) method developed by Fredrickson et al. to study the polymer/nanoparticle composites [64]. In their HPF method, the evolution of nanoparticles is calculated through BD method and the self-assembly of copolymers is simulated by SCFT method. These two hybrid modeling simulations provide hopeful routes to investigate systems in which the behaviors on different length scales are intimately and dynamically linked, such as polymer-encapsulated drugs and polymer/nanoparticle composites. However, there are still some difficulties in developing a seamless hybrid modeling strategy: primarily, an analytical expression for the force exerted by the surrounding polymers on each particle should be established; next, a reasonable coupling between the length scale and time scale of different subsystems is required. To acquire a reliable simulation results, the hybrid modeling technique combining DPD with field-theoretic methods is a recommended choice because the link between DPD interaction parameter and Flory-Huggins interaction parameter has already been established.

3. Self-assembly of linear block copolymers

The linear block copolymers are a type of copolymers consisting of two or more blocks joined in linear arrangements. Due to their broad industrial applications, the linear block copolymers have been extensively investigated in past decades [69,70]. In theoretical simulations, the linear block copolymer can be modeled as bead-spring chain [8–10] (*e.g.*, in MD) or continuous Gaussian chain [47] (*e.g.*, in SCFT) without branch. The self-assembly behaviors of the linear block copolymers in solution can be affected by the interactions among blocks and solvents, the number of blocks and the arrangement of blocks. In this section, the simulation works about the self-assembly behaviors of the linear block copolymers including AB diblock copolymers, ABA triblock copolymers and ABC triblock copolymers are reviewed. Both the morphology of self-assembled structures and the corresponding formation kinetics are discussed. Through the comparison among different linear block copolymers, the effect of molecular architecture on their self-assembly behaviors in solution is demonstrated.

3.1. AB diblock copolymers

A variety of microstructures such as spherical micelles, cylindrical micelles and vesicles can be formed through the self-assembly of AB diblock copolymers in solution. From the thermodynamic aspect, the self-assembled structure formed from AB diblock copolymers in solution strongly relies on the balance of the three contributions to the free energy: the chain stretching in the core, the interfacial tension and the repulsion interaction among coronal chains [71]. The changes of the interaction between copolymers and solvents and the block composition of copolymers would disturb the energy balance and lead to the structural transition between different self-assembled structures. In this subsection, we focus on the simulation investigations about the self-assembly of AB diblock copolymers in solution. Several significant influence factors including the solvent selectivity, the polydispersity and the chain rigidity of copolymers are discussed.

To reveal the relation between the self-assembled structures and the molecular parameters, Doi and co-workers performed a first three-dimensonal density functional theory (DFT) simulation on the self-assembly of AB diblock copolymer solutions [72]. Instead of the heuristic arguments for the expression of the density

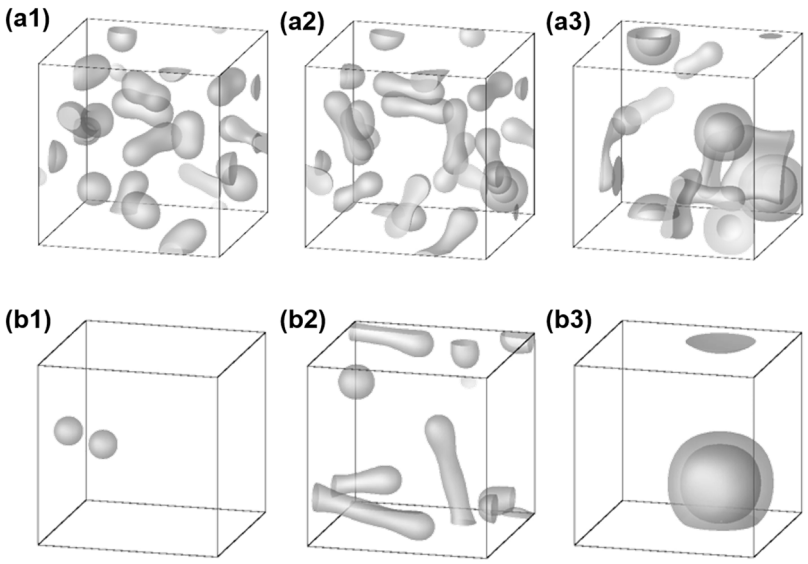

Fig. 1. (a) Self-assembled structures formed from AB diblsock copolymers in solution as a function of the solvent affinity strength of solvent-philic A blocks: (a1) $\chi_{AS} = 0.5$; (a2) $\chi_{AS} = 0$; (a3) $\chi_{AS} = -0.175$. (b) Self-assembled structures formed from AB diblock copolymers in solution as a function of the block composition of solvent-philic A blocks: (b1) $f_A = 2/3$; (b2) $f_A = 1/2$; (b3) $f_A = 2/5$. [72], Copyright 2005.
Reproduced with permission from the American Chemical Society.

functional used in earlier works [73–75], a general density functional expression involving the same parameters in SCFT has been adopted in their simulations. In their works, various self-assembled structures including spherical micelles, cylindrical micelles and vesicles have been observed as the change of the solvent affinity strength and the block composition of AB diblock copolymers, as shown in Fig. 1. The thermodynamic mechanisms underlying the structural transitions among these self-assembled structures have been concluded as below: with increasing the solvent affinity of the solvent-philic blocks, the interfacial area of the micelles tends to enlarge, and the structural transitions from spherical micelles to cylindrical micelles and then to vesicles take place, as shown in Fig. 1(a); additionally, these structural transitions can also be observed as the decrease of the block composition of the solvent-philic blocks, as shown in Fig. 1(b). Their observations of the relation between the self-assembled structures and the block composition of diblock copolymers are in agreement with the strong segregation analysis proposed by Ohta and Nonomura [76]. Another crucial influence factor of the self-assembly of AB diblock copolymers in solution is the incompatibility between the solvent-phobic blocks and the solvents. Sun et al. employed a simulated annealing method, an algorithm for searching the thermodynamic equilibrium state in polymer systems, to study the self-assembly behaviors of AB diblock copolymers in solution [77]. In their simulations, by increasing the incompatibility between the solvent-phobic blocks and the solvents, the structural transitions from spherical micelles to cylindrical micelles and then to onion-like structures have been observed. Through a quantitative analysis of the contact area among different components, they demonstrated that the structural transition from spherical micelles to cylindrical micelles is induced by the decrease of the contact area between the solvent-phobic blocks and the solvents, able to lower the total energy and stabilize the formed assemblies. Their particle-based simulations showed good agreement with the simulations presented by Doi and co-workers and experimental observations reported by Eisenberg and co-workers [78].

The above simulations demonstrate that the block composition of amphiphilic diblock copolymers strongly affects their self-assembly behaviors in solution, suggesting that the desired microstructures can be prepared by controlling the molecular weight of copolymers precisely. However, it is nearly impossible to synthesize copolymers with mono-dispersed molecular weight. And the effect of the polydispersity of copolymers on the self-assembled structures is still unclear. To solve this problem, an efficient SCFT method aiming to investigate the dependence of the self-assembled structures on the polydispersity of copolymers has been proposed by Sides and Fredrickson [79,80]. Using this SCFT method, Shi et al. studied the vesicular structures formed from amphiphilic diblock copolymers with one polydisperse block [81]. They found that the copolymers with larger polydispersity have a stronger tendency to form quasi-vesicles, in which the shorter blocks prefer to locate at the interfaces between solvent-philic and solvent-phobic blocks to minimize the stretching energy. Moreover, for the case of copolymers with polydisperse solvent-philic blocks, they concluded that the longer solvent-philic blocks tend to self-assemble into the outer layer of vesicles, that leads to a change of the spontaneous curvatures of the bilayers and then the formation of smaller vesicles. Their simulations have demonstrated the polydispersity-driven segregation mechanism of copolymers and offered a reasonable explanation for the coexist of vesicles and micelles observed in experiments [82].

The afore-mentioned studies improve our understanding of the self-assembly of flexible diblock copolymers in solution. But they do not take into account the influence of the chain rigidity of copolymers on the self-assembled structures, an important topic in polymer science [83–85]. In the early 1990s, Halperin combined scaling theory with mean-field analysis to predict the equilibrium micellar structures formed from the rod-coil diblock copolymers in solvents selective for coil blocks [86]. They predicted that the micelles with cylindrical cores and extended star-like coronas are thermodynamic stable at low rod fractions. However, they only considered the micelles with spherical geometry, and the effect of van der Waals interactions was ignored in their investigations for simplicity. In another theoretical work, Lin et al. extended Flory lattice theory to study the self-assembly of the rod-coil diblock copolymers in nonselective solvents [87]. In their extended Flory lattice model, the free energies contributed from the core-corona interface and corona region were considered. They found that the rod-coil copolymers exhibit lyotropic mesophases including lamellar, cylindrical and spherical microstructures when the volumetric

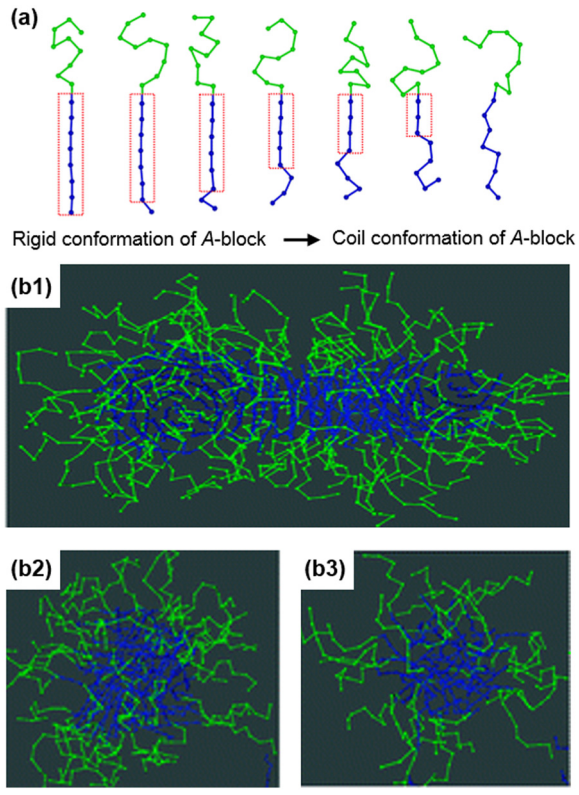

Fig. 2. (a) Layouts of A_8B_9 diblock copolymer with the A_8 block changing from a rigid conformation to coil conformation. (b) Typical snapshots of A_8B_9 copolymer systems with various percentages of the rigid conformation of A block: (b1) f_R = 100%; (b2) f_R = 71.4%; (b3) f_R = 42.9%. The blue and green colors are assigned to A and B blocks, respectively. [89], Copyright 2008. (For interpretation of the references to colour in this figure legend, the reader is referred to the web version of this article.).
Reproduced with permission from the American Chemical Society.

fraction of copolymers exceeds a critical value. And they suggested that the isotropic to anisotropic phase transition is determined by the tendency of the rod blocks to form orientational ordered arrangement.

In a recent study, Lin et al. utilized BD method to investigate the self-assembled structures and molecular packing of rod-coil diblock copolymers in solution [88]. In their simulations, the rod-coil copolymer is modeled as a linear chain consisting of several beads connecting through bond stretching potential. And the rigidity of the rod blocks is simulated by the harmonic angle bending potential $U_{\text{angle}}(\theta)$, represented by a cosine harmonic function of the orientational angle θ defined by three connected beads. Using this approach, the influence of the segregation strength between different rod blocks on the micellar structures formed from rod-coil copolymers has been studied. They found that the disk micelles with a smectic-like phase in the solvent-phobic core emerge when the rod pair interaction strength is strong enough. Moreover, a novel string micellar structure with helically packed rod blocks in the solvent-phobic core was observed in their simulations as the decrease of the rod pair interaction strength, that suggests a new route to prepare helix superstructures. With further decreasing the strength of the rod pair interaction, the rod-coil copolymers assembled into small aggregates instead of the string micelles. The effect of chain rigidity on the micellar structures formed from rod-coil diblock copolymers has been discussed in their further investigations [89,90]. A series of rod-coil copolymers with various rigid conformation fractions and rigid portion locations have been constructed, as illustrated in Fig. 2(a). As the decrease of the rigid conformation fraction, a structural transition from cylindrical to spherical micelles was observed, as shown in Fig. 2(b). These results successfully reproduce their experimental observations and suggest that the rigid conformation fraction of the rod-coil copolymers has an important effect on the self-assembled structures [89].

The block rigidity of rod-coil copolymers also plays a significant role in the formation of vesicles. By DPD method, Lin et al. constructed the morphological phase diagram of rod-coil diblock copolymers as functions of the length of rod block and the length of coil block, as shown in Fig. 3(a) [91]. According to the morphological phase diagram, they suggested that a short rod block or a weak rod–rod stacking is in favor of the formation of vesicles because a strong rod–rod stacking can impede the bending of membrane and thus the formation of vesicles. By decreasing the rod–rod interactions strength, a smectic-isotropic phase transition has been found in their simulations, in agreement with the BD simulations performed by Lin and co-workers [88–90]. Moreover, they studied the fusion between two vesicles and demonstrated that the membrane tension $\tau_m{}^0$ is significantly important on the fusion process of vesicles. They found that the fusion process of rod-coil vesicles can be divided into four stages: kissing, adhesion, hemifusion and fusion, as illustrated in Fig. 3(b). And a high membrane tension was found to be in favor of the fusion of the rod-coil vesicles. Their investigations are meaningful for us to understand the vesicle fusion process that is ubiquitous in vivo.

Although the above-mentioned simulation techniques have shown their power in studying the self-assembly of copolymer solutions, they still have some inherent limitations. For instance, the size of system that can be simulated by atomistic methods such as MD is much smaller than that by mesoscopic methods such as SCFT, and there are few investigations of the self-assembly of rod-coil block copolymers in solution by field-theoretic methods because the mathematical treatment of a semi-flexible chain model is much more complicated than that of a flexible chain model. Nevertheless, there are many promising routes to get rid of these limitations. For instance, several SCFT methods with semi-flexible or wormlike chain model have been developed to study the phase behaviors of rod-coil copolymer melts [92–94], that can be extended to rod-coil copolymer solutions in a straightforward way.

3.2. ABA triblock copolymers

Compared with the AB diblock copolymer, the ABA triblock copolymer has an additional middle block, that has a restricting effect on the other two blocks and leads to some complex structures. For example, Agrawal et al. prepared flower-like micelles through the self-assembly of poly(lactide-*b*-ethylene oxide-*b*-lactide) (PLA-*b*-PEO-*b*-PLA) solutions [95]. In their experiments, the solvent-phobic PLA blocks act as bridging chains between adjacent micelles, that leads to an entropic attraction and the formation of the flower-like micelles. In most simulation models, the ABA triblock copolymer can be classified as solvent-(philic-phobic-philic) (PHP) type and solvent-(phobic-philic-phobic) (HPH) type. In this subsection, the simulation works about the self-assembly of these two kinds of ABA triblock copolymers in solution are presented.

The ABA triblock copolymer with PHP sequence can be considered as a connection of two amphiphilic AB diblock copolymers by their solvent-phobic blocks. This imaginary connecting restricts the chain stretching in solvent-phobic core and results in the formation of some complex structures. Combining experimental techniques and SCFT simulations, Lin et al. investigated the self-assembly behaviors of poly(L-glutamic acid-*b*-propylene oxide-*b*-L-glutamic acid) (PLGA-*b*-PPO-*b*-PLGA) triblock copolymers in solution [96]. To simulate the change of the molecular weight and the secondary structure of PLGA blocks, a series of ABA triblock copolymer models with different values of the block composition f_A and the statistical length a_A of A blocks have been constructed in their SCFT

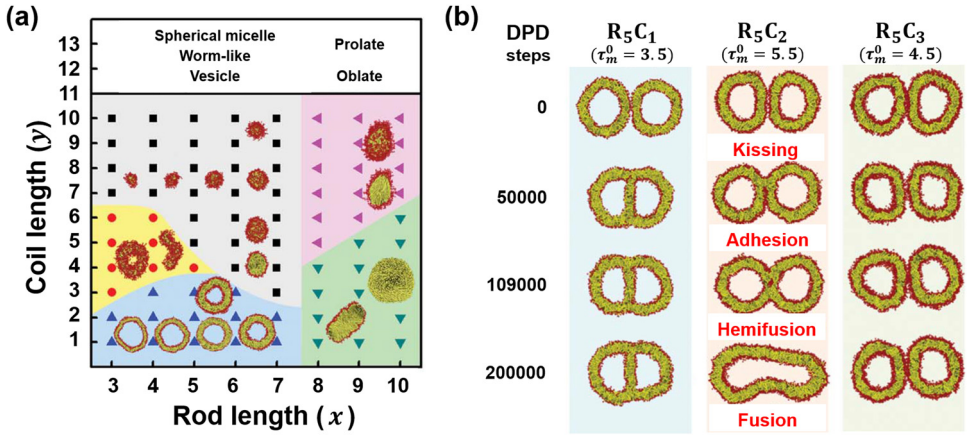

Fig. 3. (a) The morphological phase diagram of rod-coil copolymer R_xC_y as functions of rod length x and coil length y. (b) The sliced images of the fusion process for vesicles formed from rod-coil copolymer R_5C_y with $y = 1, 2, 3$. The yellow and red colors are assigned to rod R and coil C blocks, respectively. [91], Copyright 2013. (For interpretation of the references to colour in this figure legend, the reader is referred to the web version of this article.)

Reproduced with permission from the Royal Society of Chemistry.

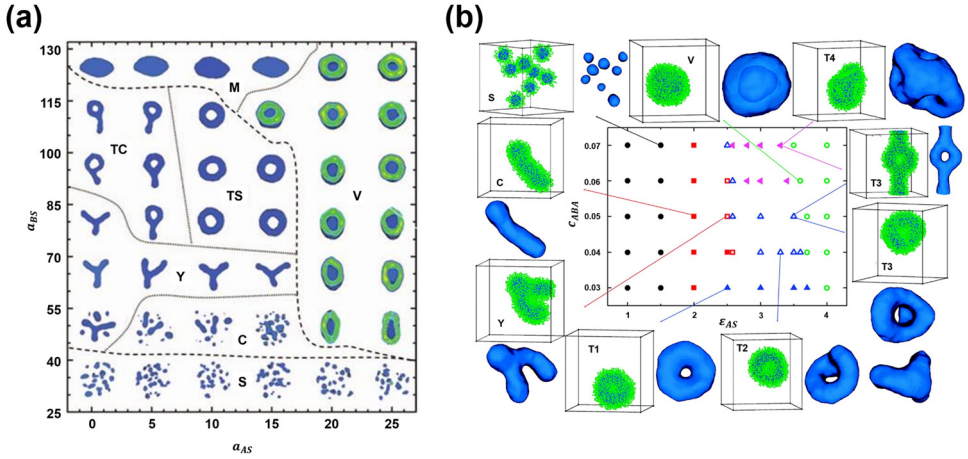

Fig. 4. (a) Morphological phase diagram of PHP type of ABA triblock copolymers as functions of DPD interaction parameters a_{AS} and a_{BS}. [97], Copyright 2010. Reproduced with permission from the American Institute of Physics. (b) Morphological phase diagram of HPH type of ABA triblock copolymers as functions of the MC interaction parameter ε_{AS} and the volumetric fraction of copolymers c_{ABA}. [100], Copyright 2010.

Reproduced with permission from the American Chemical Society.

simulations. Their simulations demonstrated that the ABA triblock copolymers with lower value of f_A or a_A tend to self-assemble into vesicular structures, coincident with their experimental observations. In addition to these vesicular structures, the ABA triblock copolymers can also self-assemble into some complex structures such as toroidal micelles and "Y" junctions. He et al. employed DPD method to study these complex microstructures formed from ABA triblock copolymers with PHP sequence in a dilute solution [97]. They found that the control of solvent selectivity is crucial to determine the self-assembled structures of ABA triblock copolymers. By varying the selectivity of solvents for different blocks, a variety of microstructures including spherical micelles (S), cylindrical micelles (C), Y-like junctions (Y), toroidal micelles (TS, TC), vesicles (V) and disk-like membranes (M) were observed, and a diagram of different self-assembled structures has been plotted, as shown in Fig. 4(a). Based on the energetic analysis proposed by Fromherz [98], they suggested that the growth of the surface tension or the reduction of the bending elasticity of a disk-like membrane can lead to a structural transition from disk-like membrane to vesicle. The energy variation underlying the structural transition is helpful in understanding the self-assembly behavior of ABA triblock copolymers.

Similar to the PHP type of ABA triblock copolymer, the HPH type of ABA triblock copolymer can be considered as a connection of two AB diblock copolymers by their solvent-philic blocks. In this case, the middle solvent-philic blocks can act as bridges when the two end blocks segregate into different solvent-phobic cores, or loops when the end solvent-phobic blocks are in the same micelle [99]. Combining the lattice MC method with the simulated annealing technique, Kong et al. systematically investigated the effects of the volumetric fraction of copolymers c_{ABA} and the interaction parameter between solvents and A blocks ε_{AS} on the self-assembled morphologies formed from HPH type of ABA triblock copolymers [100]. A rich variety of morphologies including spherical micelles (S), cylindrical micelles (C), Y-like junctions (Y), toroidal micelles (T1-T4) and vesicles (V) have been found, as illustrated in Fig. 4(b). Both loop and bridge conformations of the middle solvent-philic block have been confirmed in these self-assembled structures. They addressed that, with increasing the volumetric fraction of copolymers or the length of solvent-philic blocks, the fraction of bridge

chains increases and the formation of flower-like micelles and network structures is promoted.

Compared with the flexible ABA triblock copolymers, the self-assembly behavior of coil-rod-coil ABA triblock copolymers is more complicated because of the introduction of bond-bending energy in rod blocks. Using DPD method, He et al. studied the chain packing in toroidal micelles assembled from the PHP type of coil-rod-coil triblock copolymers [101]. They demonstrated that the solvent-phobic rod blocks adopt extended conformations in toroidal micelles, that strongly affects the shape and size of the toroidal micelles. In a recent work, Li et al. utilized BD method to investigate the effect of rod–rod attraction strength and the block asymmetry of the PHP type of coil-rod-coil copolymers on their self-assembly behaviors [102]. With decreasing the rod–rod attraction strength, the structural transitions from smectic-like disks (Fig. 5(a1)) to string micelles (Fig. 5(a2)) and then to small aggregates have been observed. Based on their BD simulations, a morphological phase diagram as functions of rod length m and rod–rod attraction strength ε_{RR} has been constructed, as shown in Fig. 5(b). It has been found that, compared with the symmetric coil-rod-coil triblock copolymers and rod-coil diblock copolymers, the asymmetric coil-rod-coil copolymers are more likely to form the long string micelles. Furthermore, they demonstrated that the coil-rod-coil copolymers suffer a larger loss of chain configuration compared with the rod-coil copolymers, that leads to a higher value of rod–rod attraction strength ε_{RR} for structural transitions. Some of their results are in good agreement with experimental observations [103–105].

The block rigidity of triblock copolymers also has an important effect on the formation of vesicles. For example, Iatrou et al. demonstrated that the triblock polypeptides with rigid middle block can self-assemble into vesicles with monolayer membrane more easily than the diblock polypeptides [106]. Employing DPD method, Lin et al. investigated the self-assembled structures formed from the PHP type of coil-rod-coil triblock copolymers with different molecular architectures [107]. In their simulations, a faceted vesicular structure that has never been reported in previous experiments or simulations was observed. They also demonstrated that, for symmetric coil-rod-coil copolymers $C_mR_xC_m$, the formation of vesicles is restricted to the regions of short coil and rod blocks because the alignment among rod blocks is unfavourable to the formation of vesicles, as illustrated in Fig. 6(a). To elevate the formation of vesicles, they constructed a model of coil-rod-coil copolymer $C_m(R_xT_y)C_m$ with a solvent-phobic T-block grafted on the solvent-phobic rod block. Since the side T-block undermines the alignment of rigid blocks and improves the crowdedness of the solvent-philic corona, the parameter region suitable for the formation of vesicles is greatly enlarged, as shown in Fig. 6(b) and (c). Their simulations provide guidance on the molecular design for the vesicle-forming copolymers.

The simulation works presented in this subsection demonstrate that various complex structures such as toroidal micelles, "Y" junctions and faceted vesicles can be formed from ABA triblock copolymers. The asymmetry of molecular architecture has proven to be influential to the self-assembled morphology. It can be inferred that, as the increase of the block number, the self-assembly behavior of linear block copolymers would be more complicated. Therefore, there is an urgent need to use theoretical simulation techniques to assist the experimental studies. Both particle-based techniques [97,98,100–107] and field-theoretical methods [96] have been successfully applied to help experimentalists in understanding their observations. An example in this subsection is the investigation combined experiments with SCFT simulations proposed by Lin and co-workers [96]. In the future, the collaboration between simulations and experiments is a promising way to prepare advanced materials from "bottom-up" approaches. However, the interaction potential in simulations should be modified to simulate the specific systems in experiments, that requires further developments of the mapping techniques [19–21].

3.3. ABC triblock copolymers

As a kind of copolymers consisting of three immiscible components, ABC linear triblock copolymers have the ability to generate a rich variety of multicompartment micelles comprising a solvent-philic shell and a segregated solvent-phobic core. For instance, Gohy et al. reported the core-shell-corona micellar structures self-assembled from poly(styrene-*b*-2-vinylpyridine-*b*-ethylene oxide) (PS-*b*-P2VP-*b*-PEO) in aqueous solution [108]. As another example, Ma et al. have prepared the bumpy-surfaced multicompartment micelles through the self-assembly of poly(styrene-*b*-butadiene-*b*-2-vinylpridine) (PS-*b*-PB-*b*-P2VP) triblock copolymers in solvents selective for P2VP [109]. However, due to the wide parameter space of the ABC triblock copolymer solutions, it is still a challenge for experimental researchers to explore all the supramolecular structures formed from the ABC triblock copolymers and reveal the underlying self-assembly principles. Several simulation techniques including SCFT [109–112], DPD [113–120] and MC [121–123] have been applied to study the self-assembly of ABC triblock copolymers in solution. Similar to the ABC triblock copolymers, the ABC triblock copolymers can be classified as PHH, HPH and PHP types according to the solvent selectivity. In the present subsection, the recent simulations of all the three types of ABC triblock copolymers have been featured.

The PHH type of ABC triblock copolymers can self-assemble into a rich variety of multicompartment micelles including core-shell-corona micelles [108,124–126] and raspberry-like micelles [127–130]. The mechanism underlying the formation of these multicompartment micelles is an important topic in this field. Using DPD method, Jiang et al. studied the structural evolution from concentric core-shell-corona micelles to raspberry-like multicompartment micelles formed from the ABC triblock copolymers in A-selective solvents [113]. The length and the solubility of B blocks were found to be crucial to the formation of raspberry-like micelles. From the thermodynamic aspect, they proposed two mechanisms about the formation of raspberry-like micelles, as illustrated in Fig. 7(a). The formation of B-bump-C micelles is entropy-driven and occurs when the length of B blocks is short, whereas the formation of C-bump-B micelles is enthalpy-dominated and takes place when the solubility of B blocks is relative low. In another work, Ma et al. studied the raspberry-like micelles formed from ABC triblock copolymers both in simulations and experiments [109,110]. The raspberry-like micelles observed in experiments were successfully reproduced in their SCFT simulations. Furthermore, they found that the energy from entropy of the spherical raspberry-like micelle ($\chi_{BS}N = 50$) is markedly higher than that of the cylindrical raspberry-like micelle ($\chi_{BS}N = 35$), as shown in Fig. 7(b). And the interfacial energy of the spherical raspberry-like micelle is considerably lower than that of the cylindrical raspberry-like micelle. Their SCFT calculations indicated that the morphology of raspberry-like micelle is determined by the competition between the enthalpy and entropy, in line with the mechanisms presented by Jiang and co-workers [113].

In addition to the PHH type of ABC triblock copolymers, the HPH type of ABC triblock copolymers are also able to self-assemble into hierarchical structures. For instance, Laschewsky et al. reported the raspberry-like micelles formed from poly(1H,1H,2H,2H-perfluorodecyl acrylate-*b*-oligoethylene glycol acrylate-*b*-2-ethylhexyl acrylate) (PFDA-POEGA-PEHA) terpolymers [128]. In a recent SCFT simulation, Wang et al. investigated the self-assembly of ABC triblock copolymers in solvents selective for the middle blocks [112]. A variety of microstructures including

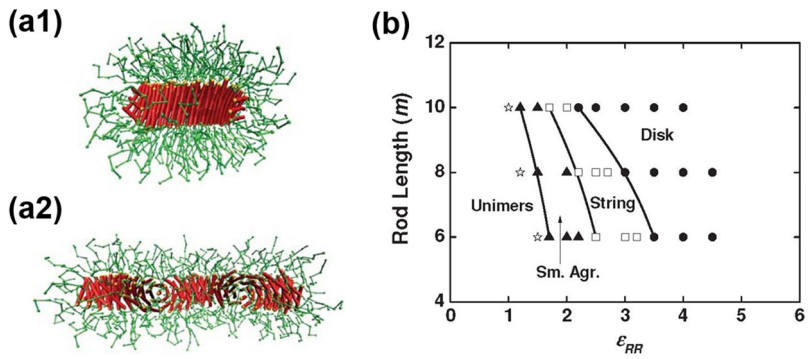

Fig. 5. (a) Typical snapshots of coil-rod-coil $A_6B_6A_6$ copolymer systems with various values of rod–rod attraction strength ε_{RR}: (a1) ε_{RR} = 3.5; (a2) ε_{RR} = 3.0. The green and red colors are assigned to coil A and rod B blocks, respectively. (b) Morphological phase diagram of coil-rod-coil $A_6B_6A_6$ copolymers as functions of rod–rod attraction strength ε_{RR} and rod length m. [102], Copyright 2011. (For interpretation of the references to colour in this figure legend, the reader is referred to the web version of this article.) Reproduced with permission from the American Institute of Physics.

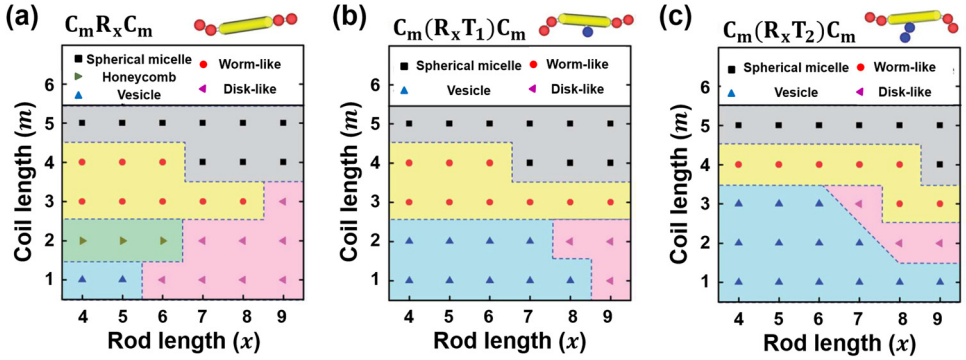

Fig. 6. (a) The morphological phase diagram of symmetric $C_mR_xC_m$ copolymers as functions of rod length x and coil length m. (b) The morphological phase diagram of T-tethered symmetric $C_m(R_xT_1)C_m$ copolymers. (c) The morphological phase diagram of T-tethered symmetric $C_m(R_xT_2)C_m$ copolymers. [107], Copyright 2014. Reproduced with permission from the Royal Society of Chemistry.

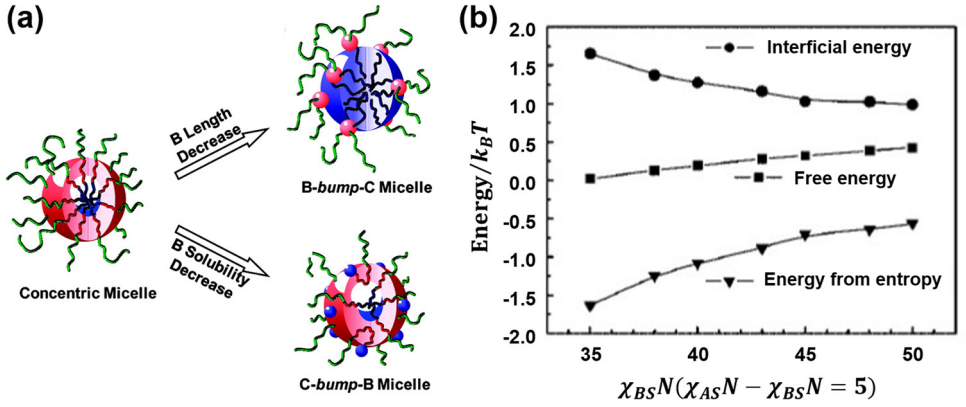

Fig. 7. (a) Sketch of morphological evolutions of multicompartment micelles formed from ABC copolymers in A-selective solvents. [113], Copyright 2011. Reproduced with permission from the American Chemical Society. (b) The free energy of raspberry-like micelles as a function of $\chi_{BS}N$ calculated by SCFT. [109], Copyright 2009. Reproduced with permission from the American Chemical Society.

spherical micelles with A and C helix-like cores (HHS), spherical micelles with A and C disk-like cores (DDS), cylindrical micelles with A ring-like core and C disk-like core (RDC), cylindrical micelles with A and C ring-like cores (RRC), cylindrical micelles with A spherical core and C cylindrical core (SCC), spherical micelles with A and C spherical cores (SSS) and special vesicles with A tube-like core (SV) have been observed. And a triangular morphological phase diagram as functions of the block composition of each block has been summarized, as represented in Fig. 8(a). In their simulations, the compartmentalized raspberry-like micelles reported by Laschewsky et al. [128] have been confirmed. Moreover, an interesting finding in their investigations is the double-stranded superhelix structure in which the A and C blocks form alternate helices and the B blocks organize into the shell, as shown in Fig. 8(b). Based on the free energy calculations, the thermodynamic stability of the superhelix structure has been confirmed, as shown in Fig. 8(c). Through a detailed energy analysis of the interaction enthalpy and the configurational entropy, they demonstrated that the formation of superhelix is beneficial to the relaxation of chain stretching but results in unfavourable interaction enthalpies. These theoretical simulations of the HPH type of ABC triblock copolymers offer guidance for preparing multicore micelles.

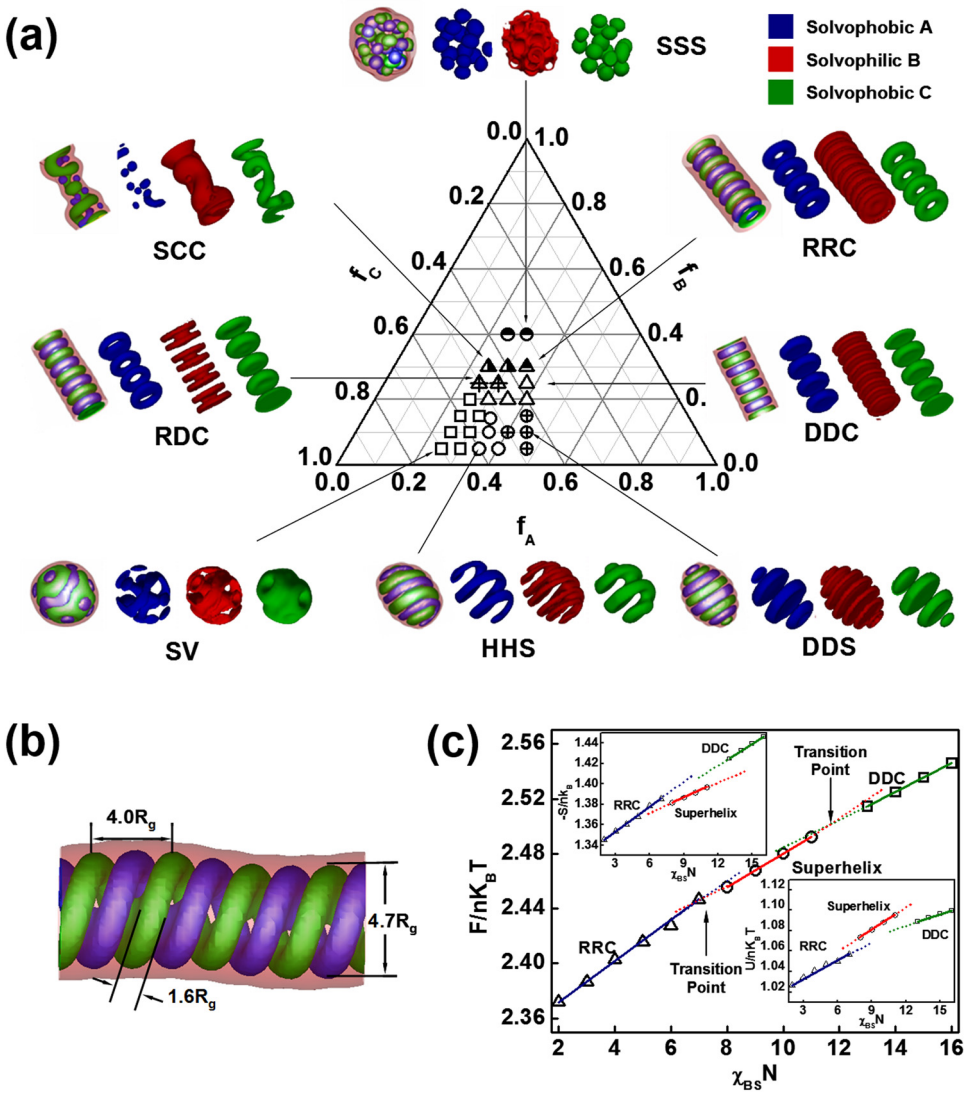

Fig. 8. (a) Triangular morphological phase diagram of the HPH type of ABC triblock copolymers as functions of the block compositions of the A, B and C blocks (f_A, f_B and f_C). (b) The double-stranded superhelix structure with diameters of approximately 4.7R_g and a pitch of approximately 4.0R_g. (c) The plots of free energy F, configurational entropy S and internal energy U as a function of $\chi_{BS}N$ for various microstructures. The blue, red and green colors are assigned to solvent-phobic A, solvent-philic B and solvent-phobic C blocks, respectively. [112], Copyright 2011. (For interpretation of the references to colour in this figure legend, the reader is referred to the web version of this article.) Reproduced with permission from the Royal Society of Chemistry.

In contrast to the ABC triblock copolymers containing two solvent-phobic blocks, the PHP type of ABC triblock copolymers is unable to form micellar structures with hierarchical solvent-phobic core. Instead, they tend to self-assemble into micellar structures with separated solvent-philic domains. Among the various microstructures formed from the PHP type of ABC copolymers, the vesicular structures with asymmetric membranes have drawn a lot of attention due to their potential biomedical applications [131–134]. Using lattice MC simulations, Cui et al. investigated the asymmetric vesicles formed from the PHP type of ABC copolymers [121]. In their simulations, the partial-reptation algorithm was adopted to enhance the efficiency of the evolution of the chain configuration. They found that the asymmetric three-layer vesicles can be formed when the incompatibility between the two kinds of solvent-philic blocks is strong. They also demonstrated that the distribution of the solvent-philic blocks can be controlled by changing the selectivity of solvents and the length of solvent-philic blocks. In a further investigation of these asymmetric vesicular structures, Li et al. performed DPD simulations to study the structural transitions among different vesicular structures formed from the PHP type of ABC copolymers [116]. Through adjusting the DPD interaction parameters a_{AA} and a_{CC}, the influence of spontaneous membrane curvature on the shape of vesicles was investigated. By comparing their simulation results with the spontaneous curvature model proposed by Herfrich [135], they derived the functional dependence of the reduced membrane curvature C_0 of the vesicles on the difference of DPD interaction parameters $\Delta a = a_{AA} - a_{CC}$, as shown in Fig. 9(a). Additionally, by changing the value of Δa, various vesicular structures have been observed, as shown in Fig. 9(b). It was found that the spherical vesicle transform into oblate or prolate vesicle when the value of Δa is relative small, in agreement with the theoretical predictions of Markvoort [136]. Furthermore, on the basis of the oblate or prolate shape, the range of vesicular structures grows larger and new shapes appear with increasing Δa. Their findings reveal a reasonable mechanism about the shape transition of vesicles and provide guidance to control the shape of vesicles in experiments.

The above simulations have significantly advanced our understanding of the self-assembly behaviors of ABC triblock copolymers in solution. Specially, the free energy analysis proposed by Wang

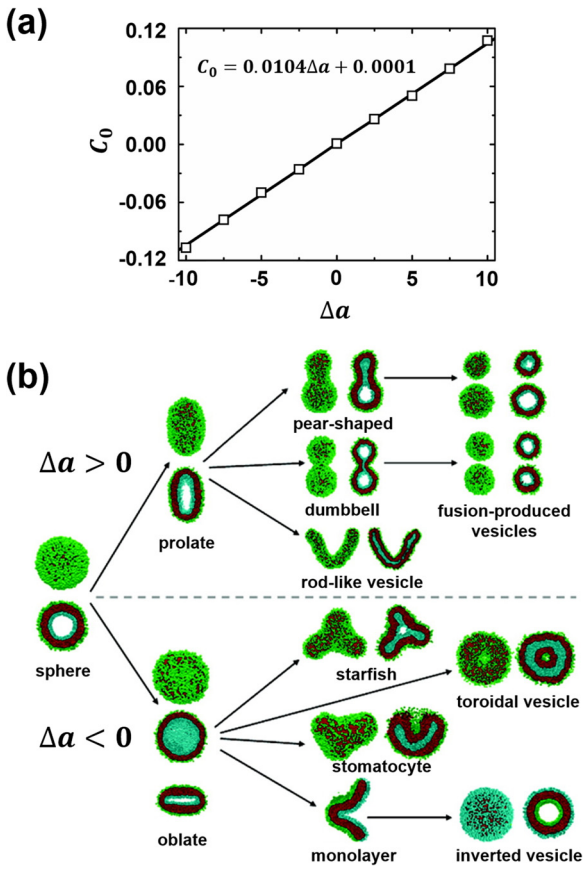

Fig. 9. (a) Relation between the spontaneous curvature C_0 of the vesicle membrane and the DPD interaction parameters $\Delta a = a_{AA} - a_{CC}$ obtained from DPD simulations. (b) Morphological transition of vesicles formed from the PHP type of ABC copolymers. The value of Δa is positive in the upper half and negative in the lower half. The red, green, blue colors are assigned to solvent-phobic B blocks, solvent-philic A blocks and solvent-philic C blocks, respectively. [116], Copyright 2009. (For interpretation of the references to colour in this figure legend, the reader is referred to the web version of this article.)

Reproduced with permission from the American Chemical Society.

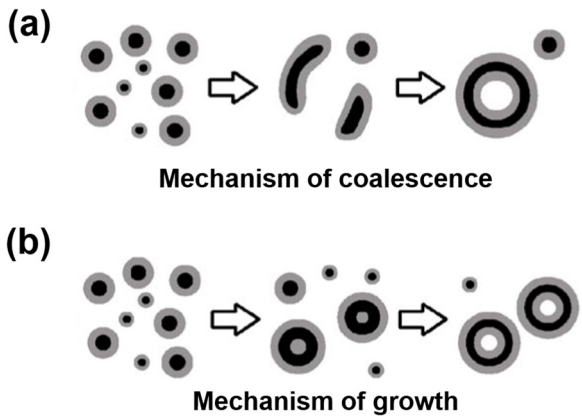

Fig. 10. Schematic representation of two vesicle formation mechanisms observed in the self-assembly process: (a) the mechanism of coalescence; (b) the mechanism of growth. [153], Copyright 2007.

Reproduced with permission from the American Institute of Physics.

et al. has enhanced our knowledge about the thermodynamic mechanism underlying the structural transition between different self-assembled structures [112]. However, the Helmholtz free energy adopted in their simulations should be employed to describe an entire macroscopic system and is unsuitable to represent a dilute solution system. To solve this problem, Wang et al. subsequently proposed an improved method to explore the free energy landscape of polymer solutions [137]. This is referred in section 4 of this review, where the self-assembly of graft copolymer solutions is considered.

3.4. Self-assembly kinetics of linear block copolymers

The above sections focus on the influence of thermodynamic factors, such as the incompatibility between different components, on the self-assembled structures formed from linear block copolymers in solution. However, the self-assembly behaviors of copolymers are determined by not only the thermodynamic factors but also the self-assembly kinetics. In an ideal situation, the morphology of copolymer assemblies can be altered not by changing the molecular parameters of copolymers but through controlling the sample preparation process [138,139]. Furthermore, the careful control of the self-assembly pathway can allow for the creation of some non-equilibrium structures, helpful for us to understand the self-assembly processes happened in organisms [140–142]. In order to take full advantage of these possibilities, one needs an in-depth understanding of the self-assembly kinetics of copolymers in solution. Over the past decades, some experimental techniques including time-resolved dynamic light scattering (DLS), small-angle neutron scattering (SANS) and X-ray scattering (SAXS) have been applied to study the formation kinetics of vesicles, and an intermediate state consisting of disk-like micelles were captured [143,144]. As an efficient and economic alternative, theoretical modeling and simulation are powerful for studying the formation kinetics of self-assembled structures. The kinetics of the micellization of block copolymers have been reviewed elsewhere [145]. In this subsection, we focus on the formation kinetics of vesicles and some complex micellar structures formed from linear block copolymers. The influence of the volumetric fraction of copolymers, the solvent selectivity and the hydrodynamic force on the formation pathway of the self-assembled structures is discussed in detail.

Among the various assemblies formed from copolymers in solution, the vesicular structures have attracted tremendous attention due to their biological significance [146,147]. Several computer simulation methods have been fruitfully applied to investigate the formation process of a vesicle. Two formation mechanisms of vesicles including mechanism of coalescence [148–150] and mechanism of growth [151–153] were found in these simulations, as shown in the schematic of Fig. 10. For the mechanism of coalescence, the vesicles are formed as follows: firstly, the amphiphilic block copolymers aggregate into small spherical micelles; then the micelles coalesce to bilayer membranes (or oblate micelles); finally, the bilayers bend and close up to form a vesicle. For the mechanism of growth, the small micelles do not coalesce but simply grow to quasi-vesicles (big micelles with a solvent-philic core) and then the vesicles. In these simulations, it has been found that several factors such as the volumetric fraction of copolymers and the solvent selectivity are crucial to control the formation pathway of vesicles. Using lattice dynamic MC simulations, Huang et al. studied the influence of solvent selectivity on the formation process of the vesicles self-assembled from AB diblock copolymers [154]. In their simulations, an improved bond fluctuation model with the bond length between sequentially linked beads from 1 to 3 has been adopted to describe the copolymer solutions. The solvent selectivity characterized by the interaction parameter between solvent-phobic B beads and solvents ε_{BS} was found to be a key factor to control the formation pathway of vesicles. For a small ε_{BS}, the mechanism of coalescence has been observed. While for a large ε_{BS}, the vesicle was found to be formed through the mechanism of growth. They

also demonstrated that the size of vesicles can be regulated through the incompatibility between solvent-phobic B beads and solvents.

The formation pathway of the self-assembled structures is also affected by the volumetric fraction of copolymers. He et al. employed EPD method to study the structural formation kinetics of amphiphilic AB diblock copolymers in solution [151,152]. In their simulations, the incompatibility among different blocks and solvents are characterized by the Flory-Huggins parameters χ_{IJ}, and the volumetric fraction of copolymers c_{AB} is a conserved quantity. The morphological phase diagram of final self-assembled structures including vesicles (V), ring-like micelles (T1), toroidal micelles (T2) and mixture of rod-like and spherical micelles (RS) as functions of the volumetric fraction of copolymers c_{AB} and the solvent affinity strength of solvent-philic B blocks χ_{BS} has been constructed, as shown in Fig. 11(a). In addition, they found that the formation pathway of self-assembled structure depends on the values of c_{AB} and χ_{BS}. As illustrated in Fig. 11(a), for each self-assembled structure, the dashed line separates different regions where the structure formation proceeds along different pathways: pathway of coalescence in the regions RS1 and V1, pathway of growth in the regions RS2, V2, T1 and T2. Furthermore, as illustrated in Fig. 11(b), they found that the incubation times τ^* of different micellar structures follow a single power law function of $1/\tau^* = A(\chi_{BS} - \chi^*)\alpha$, where the exponent $\alpha \approx 1.25$ and $\chi^*(c_{AB}) = 1.3 - 11c_{AB}$. In their EPD simulations, this power law behavior has been verified in a wide range of c_{AB} regardless of the type of the final structure and the related formation pathway, that indicates that the characteristics of the initial stage of self-assembly are universal and can be explained by the spinodal-type instability. Their simulations showed that the EPD is a powerful method to study the self-assembly kinetics of copolymer systems. Based on their simulations, several methods have been proposed to control the kinetic traps in the self-assembly process and the final self-assembled structures [155].

Although the EPD method is approximately valid to simulate the Rouse-type chain dynamics [47,62], it neglects the effect of hydrodynamic interactions. The long-range hydrodynamic interactions have been confirmed to be able to influence the formation kinetics of the ordered microstructures in melts [156,157]. Nevertheless, for the copolymers in solution, the effect of hydrodynamic interactions on the self-assembly kinetics is still unclear. In a recent work, Zhang et al. proposed a hybrid numerical method that combines the lattice Boltzmann method with the dynamic SCF method to study the influence of hydrodynamic interactions on the formation process of vesicles in diblock copolymer solutions [158]. In their simulations, the dynamic SCF equations are solved through a finite difference scheme [159–161], and the continuity equation and the Navier-Stokes equations are solved through the multiple-relaxation-time lattice Boltzmann method [162,163]. As presented in Fig. 12(a) and (b), by calculating the time evolution of the free energy density $\upsilon_0 F/(k_B TV)$ and the segregation parameter S, they demonstrated that the hydrodynamic interactions significantly help the system overwhelm the free energy barriers and achieve the final equilibrium state. They also found that the accelerating effect of the hydrodynamic interactions is stronger for systems with smaller shear viscosity η_s. In addition to the accelerating effect, the hydrodynamic interactions also contribute to determining the formation pathway of vesicles. In their simulations, the formation pathway of coalescence has been observed in systems without hydrodynamic flows, and the formation pathway of growth was observed when the convective flow was turned on, as illustrated in Fig. 12(c) and (d). Through the Minkowski functional analysis of the self-assembled structures [164], they concluded that the spherical intermediates are favored when hydrodynamic interactions exist, that explains the preference of the formation pathway of growth. Furthermore, they investigated the effect of hydrodynamic interactions on the fusion of vesicles. The typical stake-pore fusion mechanism has been observed [165], and the fusion process was found to be accelerated by the hydrodynamic interactions.

In the field of self-assembly of copolymers in solution, an important issue is how to control the formation pathway of the self-assembled structures by adjusting the molecular parameters or changing the experimental conditions. The above-cited simulation techniques including the particle-based methods and the field-theoretical methods have been successfully applied to study the influence the volumetric fraction of copolymers, the solvent selectivity and the hydrodynamic force on the formation pathway of the self-assembled structures. Nevertheless, the effect of block rigidity on the self-assembly kinetics of copolymer solutions has been ignored in existing simulations. Furthermore, a future topic in this field is to prepare hierarchical superstructures from linear copolymer assemblies through a way similar to the polymerization reaction. For example, the "colloidal polymer" formed from the assemblies of linear ABC copolymers has been reported by Gröschel and co-workers [166]. However, it is still a challenge to measure the "reaction kinetics" of this process by experimental techniques. The theoretical simulation provides a powerful tool to investigate the underlying mechanism and establish the "reaction kinetics" of this "colloidal polymerization" process.

4. Self-assembly of graft copolymers

Similar to linear copolymers, the self-assembly of graft copolymers in solution is also dominated by the competition between the chain stretching energy in the core, the interfacial energy and repulsion energy among coronal chains [71]. However, the branched architecture makes the self-assembly behaviors of graft copolymers more complicated. For example, some distinct properties such as the worm-like behavior, seldom observed in the linear copolymer systems, can be found in graft copolymer systems [167]. These unusual self-assembly behaviors of graft copolymers offer opportunities for new applications possible and have drawn tremendous attention. The self-assembly of graft copolymers in solution can be conceived as below: on one hand, the phase separation between side chains and backbone occurs at each grafting position; on the other hand, the backbone interconnects the local structures together into the final structures, sometimes hierarchical structures. In this section, the simulations of the intramolecular and intermolecular self-assembly of AB graft copolymers are presented. In particular, the hierarchical vesicular structures formed from graft copolymers and the corresponding formation kinetics are discussed in detail.

4.1. AB graft copolymers

Graft copolymers can self-assemble into both intramolecular and intermolecular assemblies in selective solvents. Through MD simulations and scaling theory, the intramolecular structures formed from amphiphilic graft copolymer with solvent-phobic backbone have been studied by Kosovan and co-workers [168]. In their simulations, the "pearl-necklace" assemblies resulted from the competition between the repulsive and attractive intramolecular interactions have been found. And they demonstrated that the size of pearls can be regulated by adjusting the intramolecular interactions among grafts. However, their simulations assumed that the solution of graft copolymers is infinite dilute so that intermolecular interactions can be neglected, unsuitable in most cases. Zhang et al. performed SCFT calculations on the intermolecular assemblies formed from AB graft copolymers in solution [169]. In their simulations, the graft copolymers with solvent-phobic backbone and solvent-philic backbone are considered. Various microstructures including spherical micelles, cylindrical micelles,

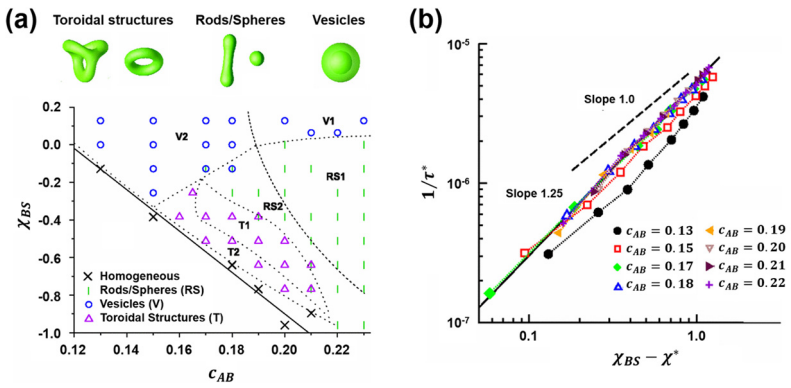

Fig. 11. (a) Morphological phase diagram of final self-assembled structures formed from AB diblock copolymers as functions of the solvent affinity strength of the solvent-philic B blocks χ_{BS} and the volumetric fraction of copolymers c_{AB}. (b) Inverse incubation time $1/\tau^*$ as a function of χ_{BS} for different volumetric fractions of copolymer. [152], Copyright 2008.

Reproduced with permission from the American Physical Society.

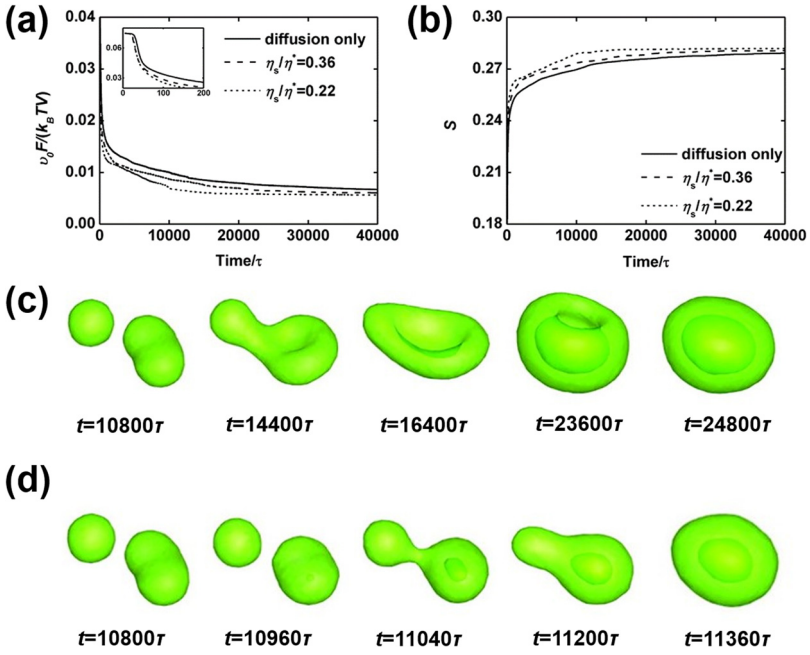

Fig. 12. Time evolution of (a) the free energy density $\upsilon_0 F/(k_BTV)$ and (b) the segregation parameter S during the quenching process of AB diblock copolymers in solution. The inset in (a) shows the time evolution of free energy density in the initial stage. Representative snapshots during the formation process of a vesicle: (c) the hydrodynamic interaction is turned off all the time; (d) the hydrodynamic interaction is turned on at time of 10800τ. [158], Copyright 2011.

Reproduced with permission from the American Chemical Society.

large compound micelles and vesicles have been observed. It was found that the architectural parameters, such as the graft density and the location of graft points, have a significant influence on the intermolecular assemblies formed from AB graft copolymers. This structural transition induced by architectural parameters has also been observed by Qi et al. through a three-dimensional DFT simulation [170]. Moreover, several complex structures including toroidal micelles, cage-like micelles and "sphere-in-vesicle" nanostructures have been found. The simulations carried out by Qi and co-workers confirmed the ability of AB graft copolymers to self-assemble into complex micellar structures.

In addition to the complex micellar structures, the AB graft copolymers are also capable to self-assemble into hierarchical vesicles such as the multilamellar vesicle (MV). Using DPD method, Chang et al. studied the self-assembly behaviors of graft copolymers in solvents selective for side chains [171]. Fig. 13(a) illustrated the influences of the volumetric fraction of copolymers c and the solvent affinity strength of solvent-philic A blocks a_{AS} on the self-assembled structures. They demonstrated that the total number of layers in MV increases with increasing the volumetric fraction of copolymers. Additionally, it has been found that the side chain length y and the gap length between adjacent side chains g strongly affect the thickness and the total number of the solvent-phobic layers in MV, as presented in Fig. 13(b). Their results successfully reproduced the experimental observations reported by Li and co-workers [172]. However, neither their simulations nor relevant experiments have confirmed the thermodynamic stability of MV formed from AB graft copolymers. Recently, Wang et al. utilized SCFT to validate the thermodynamic stability of the hierarchical vesicles formed from AB graft copolymers in solution [137]. Through the grand canonical ensemble SCFT calculations, Wang et al. calculated the excess grand free energy $\Delta G=(G-G_{homo})$ of the

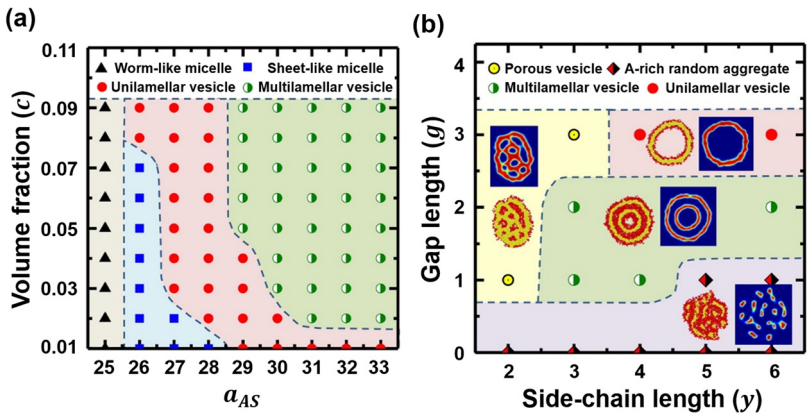

Fig. 13. (a) Morphological phase diagram of B_{11}-g-$(A_4)_3$ copolymers as functions of the volumetric fraction of copolymers c and the solvent affinity strength of solvent-philic A blocks a_{AS}. (b) Morphological phase diagram and characteristic snapshots of B_{11}-g-$(A_y)_n$ copolymers at $c = 0.05$ and $a_{AS} = 29$ as functions of the side-chain length y and the gap length g. The red and yellow colors are assigned to solvent-philic A side chains and solvent-phobic B backbones, respectively. [171], Copyright 2013. (For interpretation of the references to colour in this figure legend, the reader is referred to the web version of this article.)
Reproduced with permission from the American Chemical Society.

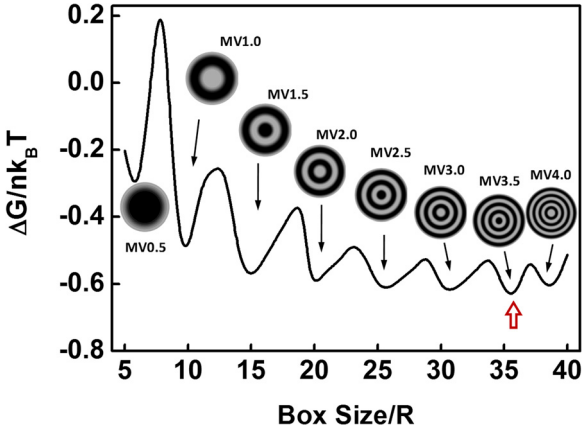

Fig. 14. Excess grand free energy of the graft copolymer systems containing MV as a function of the simulation box size which corresponds to the associated number of AB graft copolymers. The red arrow features the global minimum value of the excess grand free energy. [137], Copyright 2013. (For interpretation of the references to colour in this figure legend, the reader is referred to the web version of this article.)
Reproduced with permission from the Royal Society of Chemistry.

hierarchical vesicle systems, where G_{homo} is the grand free energy of homogenous solution. In their simulations, the excess grand free energy of the graft copolymer solutions as a function of the associated number of graft copolymers has been calculated, as shown in Fig. 14. The microstructures are labeled by MVn where n represents the number of bilayers: n=0.5 means a micelle, n=1.0 means a unilamellar vesicle, n=1.5 means a MV comprising a micelle within a unilamellar vesicle, and so on. They found that the MV structures have lower excess grand free energy than spherical micelle and unilamellar vesicles when the associated number of graft copolymers is high enough. Their SCFT calculations suggested that the multilamellar vesicle MV3.5 (one micelle within three concentric vesicles) possesses a global minimum excess grand free energy, as indicated by the red arrow in Fig. 14. Furthermore, they demonstrated that, for systems far beyond critical micelle concentration (CMC), the AB graft copolymers self-assemble into transient aggregates without the process of overcoming an activation barrier, in consistent with the argument about linear amphiphilie systems proposed by Besseling and co-workers [173]. The above investigations indicate that the AB graft copolymer solutions are promising systems with capability to prepare stable hierarchical vesicles.

When the AB graft copolymer comprises a rigid backbone, some special types of graft copolymer including T-shaped copolymer, that consists of a rigid backbone and one side chain, and π-shaped copolymer, that consists of a rigid backbone and two side chains, are formed. Employing BD method, Kim et al. investigated the micellar structures formed from T-shaped graft copolymers in solvents selective for the flexible side chains [174]. In their simulations, the structural transitions from spherical micelles to cylindrical micelles then to wire-like micelles were observed through increasing the rigidity of the backbone. By DPD simulations, Chen et al. reported the various microstructures generated by π-shaped copolymers in solution [175]. They found that the distance between junction points affects the steric repulsion between micelles and then the morphology of assemblies. By tailoring the distance between junction points and the interaction parameters between the coil and rod blocks, the cage-like micelles and network structures that have potential applications in drug delivery can be formed.

Through simulations, the influences of molecular architecture, solvent selectivity and chain rigidity on the self-assembly of graft copolymer solutions have been studied. Moreover, and the thermodynamic stability of the hierarchical vesicular structures has been confirmed by theoretical simulations. These simulations demonstrated that the graft copolymer systems are promising candidates to prepare hierarchical structures. However, the self-assembly behaviors of graft copolymers with rigid blocks as backbone or side chains are still not well studied. For example, the rod-coil poly(γ-benzyl-L-glutamate-*g*-ethylene glycol) (PBLG-*g*-PEG) graft copolymers are found to be capable of forming connected-spindle through a hierarchical self-assembly strategy [176]. The underlying mechanism of this novel structure is still unclear, and the theoretical simulation may provide an opportunity to investigate this superstructure.

4.2. *Self-assembly kinetics of graft copolymers*

As a type of branched copolymers in which the grafts are chemically distinct from the backbone, even the simplest AB graft copolymers can self-assemble into hierarchical structures. The hierarchical structures formed from the graft copolymers, such as the multilamellar vesicle mentioned in section 4.1, have attracted great attention because of their biological significance. However, there exist many confusing issues about the formation kinetics of these hierarchical structures. For instance, does the phase

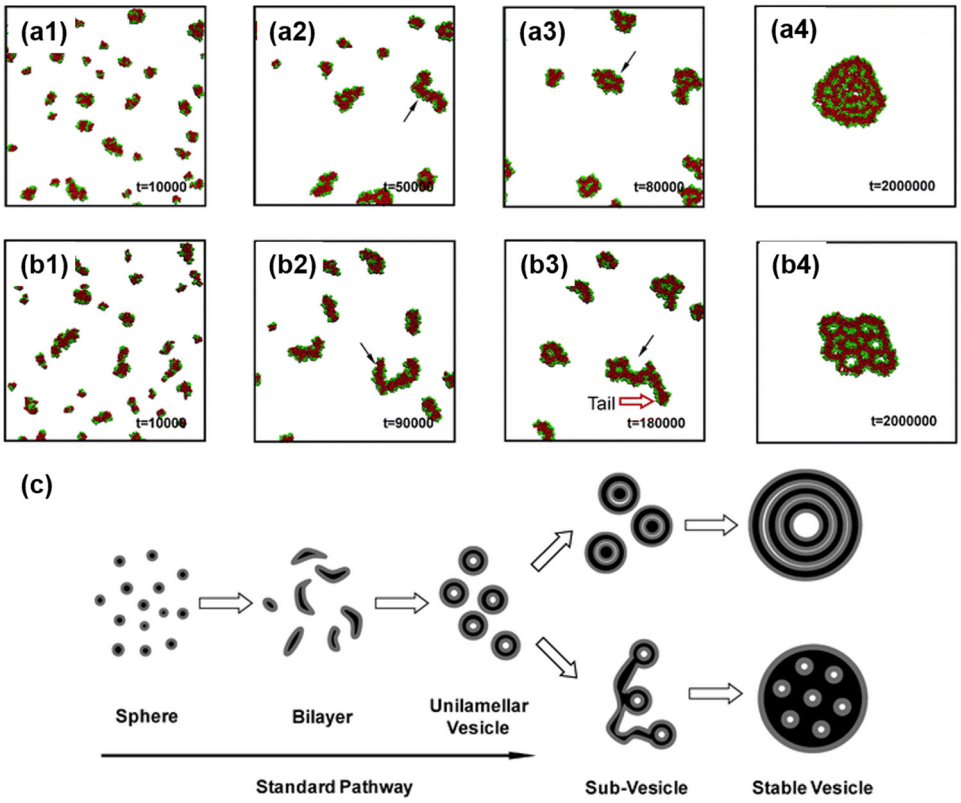

Fig. 15. (a) Formation pathway of the multilamellar vesicle: (a1) $t = 10000$; (a2) $t = 50000$; (a3) $t = 80000$; (a4) $t = 2000000$. (b) Formation pathway of the large-compound vesicle: (b1) $t = 10000$; (b2) $t = 90000$; (b3) $t = 180000$; (b4) $t = 2000000$. The green and red colors are assigned to the solvent-philic backbones and solvent-phobic graft arms, respectively. The black arrows indicate the representative structures. (c) Sketch of the formation kinetics of the hierarchical vesicles. [137], Copyright 2013. (For interpretation of the references to colour in this figure legend, the reader is referred to the web version of this article.)
Reproduced with permission from the Royal Society of Chemistry.

separations of the large-length-scale and the small-length-scale occur simultaneously, and how to prepare the desired hierarchical structures through a control over the self-assembly kinetics? Considering the similarity between hierarchical vesicle and biological cells, the answers for these issues may help us to understand the physiology of multicell organisms.

In a recent work, Wang et al. utilized DPD method to study the formation process of hierarchical vesicles formed from AB graft copolymers [137]. They found that, accompanied by the formation of multiple metastable structures, the hierarchical vesicles including multilamellar vesicles (Fig. 15(a)) and large-compound vesicles (Fig. 15(b)) are formed through a hierarchical pathway. At the beginning of the formation process of hierarchical vesicles, the graft copolymers self-assemble into unilamellar vesicles, similar to the linear block copolymers. Then the unilamellar vesicles grow into multilamellar sub-vesicles with less bilayers or coalesce into small compound sub-vesicles, analogous to the process of cell fusion observed in organisms. The growth or coalescence of these metastable sub-vesicles continues until the system achieves its equilibrium state, as illustrated in Fig. 15(c). By calculating the excess grand potential of the hierarchical vesicles, the multiple metastable states in the formation process of hierarchical vesicles have been confirmed. They suggested that these metastable states lead to the hierarchical formation process of the hierarchical vesicles. This is an important example of investigation about the formation kinetics of hierarchical vesicles, that provides useful information for a further understanding of the hierarchical structures. Due to the hierarchical property of biological cells, the formation kinetics of hierarchical vesicles may help us to explore the fusion and fission of biological cells.

5. Self-assembly of copolymers with complex architectures

In the past decades, the advanced synthetic techniques allowing for the synthesis of the copolymers with complex architectures, such as star-like copolymers [177], dendritic copolymers [178,179] and bottle-brush copolymers [180], have been rapidly matured. A lot of attention has been paid on these copolymers because they exhibit many distinct properties compared with linear block copolymers and graft copolymers. Several simulation techniques have been applied to investigate the self-assembly of these copolymers in solution. In the present section, the simulations of the star-like copolymers including A_nB_n, A_nB_m, $(AB)_n$ and ABC star-like copolymers, the dendritic copolymers and the bottle-brush copolymers are featured.

5.1. Star-like copolymers

Star-like copolymers are branched macromolecules consisting of several linear arms jointing at one junction point. Depending on the topological structure of arms, star-like copolymers are classified into symmetric A_nB_n and asymmetric A_nB_m heteroarm copolymers, $(AB)_n$ blockarm copolymers and ABC heteroarm copolymers. Some unique properties and associated applications of star-like copolymers have been discussed in a number of experimental studies. For instance, the star-like copolymers have hydrodynamic radii smaller than those of the linear copolymers with identical molecular weights [181], important for avoiding unnecessary uptake by the reticuloendothelial system in drug delivery [182]. To elucidate these experimental observations and understand the self-assembly behaviors of star-like copolymers in solution, Havránková et al.

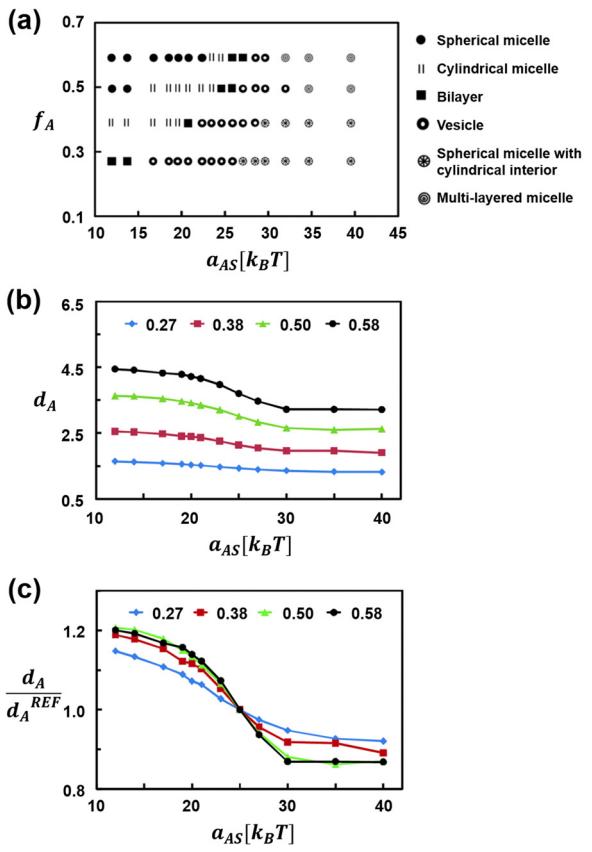

Fig. 16. (a) Morphological phase diagram of the AB_2 star-like copolymers as functions of the block composition of A arms f_A and the solvent selectivity of A arms a_{AS}. (b) The average end-to-end distance d_A of A arms as a function of a_{AS}. The d_A is evaluated as $d_A = \frac{1}{M_P}\sum_{i=1}^{M_P}|r_{i\alpha[A]} - r_{i\beta[A]}|$, where M_P is the number of AB_2 copolymer chains in the system, $r_{i\alpha[A]}$ and $r_{i\beta[A]}$ are the positions of the first bead and the last bead of the A group in the i-th molecule, respectively. (c) The relative ratios of contraction and expansion d_A/d_A^{REF} of A arms as a function of a_{AS}. [187], Copyright 2011. Reproduced with permission from the American Institute of Physics.

developed a new variant of MC algorithm to study the self-assembly of symmetric A_nB_n star-like copolymers in solution [183–185]. It was found that the association number of the micelles formed from the A_nB_n star-like copolymers with longer arms is higher. Furthermore, they confirmed that the CMC of the star-like copolymers is much higher than that of the linear copolymers. This conclusion coincides with the experiments carried out by Yun et al. [186], in which the CMC of linear poly(isobutylene-*b*-methyl vinyl ether) block copolymers measured at 23 °C is found to be lower than that of the star-like counterparts.

For asymmetric A_nB_m star-like copolymers, the length of arms has a profound influence on their self-assembly behaviors in solution. Han et al. utilized DPD method to study the effect of the arm length and the solvent selectivity for A blocks on the assemblies formed from AB_2 star-like copolymers [187]. Fig. 16(a) shows the morphological phase diagram of AB_2 star-like copolymers, divided into regions of solvent-philic A ($a_{AS} \leq 25$) and solvent-phobic A ($a_{AS} > 25$). In the solvent-philic A regions, they found that the increase of the length of A arms can lower the interfacial tension between solvents and solvent-phobic core and then lead to the structural transition from bilayers or vesicles to cylindrical or spherical micelles. On the other hand, in the solvent-phobic A regions, the interfacial tension increases with increasing the length of A arms. In particular, multi-layered micelles were observed when $a_{AS} > 30$. To investigate the dependence of the effective volume of A groups on the length of A arms, they calculated the average end-to-end distances of A groups and the relative ratios of contraction and expansion, as shown in Fig. 16(b) and (c) respectively. They found that, with increasing the length of A arms, the values of the effective volume of the A groups take a wider range and more diverse morphologies appear. Based on these results, they concluded that the AB_2 molecules with short solvent-philic A arms have a superior vesicle-forming tendency, that provides an important guidance for the synthesis of vesicle-forming copolymers.

Another typical star-like copolymer is the $(AB)_n$ or $(BA)_n$ blockarm copolymer. For these star-like copolymers, the block sequence of arms has a great influence on the resulting morphologies. Using DPD method, Sheng et al. investigated the intramolecular and intermolecular self-assembly of $(AB)_n$ and $(BA)_n$ star-like copolymers in solvents selective for A blocks [188]. They found that the tendency of $(AB)_n$ and $(BA)_n$ star-like copolymers to form intermolecular aggregates is determined by their intramolecular conformations. For $(BA)_n$ star-like copolymers with solvent-phobic B blocks as inner section, the solvent-phobic B blocks collapse into the core surrounded by the corona formed from the solvent-philic A blocks, that hinders the formation of the intermolecular assemblies. In contrast to the $(BA)_n$ star-like copolymers, the $(AB)_n$ star-like copolymers with solvent-philic A blocks as inner section tend to form intramolecular structures with a few exposed solvent-phobic B domains, that subsequently leads to the intermolecular assembly. In addition, various supramolecular structures including multicore micelles, segmented worm-like micelles and core-lump micelles can be found in systems of the $(AB)_n$ star-like copolymers. These results suggest that the intermolecular assembly of blockarm star-like copolymers can be controlled by adjusting the block sequence of arms.

The ABC heteroarm copolymers with three incompatible arms are able to self-assemble into a variety of fascinating microstructures in solution. Compared with the linear ABC triblock copolymers, the star-like architecture of the ABC heteroarm copolymers effectively promotes the formation of non-concentric multicompartment micelles. For instance, Lodge et al. successfully prepared a series of multicompartment micelles including hamburger micelles, segmented wormlike micelles and nanostructured vesicles through the self-assembly of poly(ethylethylene-*arm*-ethylene oxide-*arm*-perfluoropropylene oxide) (μ-EOF) heteroarm copolymers [189]. Through DPD simulations, Xia et al. studied the multicompartment micelles formed from ABC heteroarm copolymers [190]. In their simulations, a series of ABC heteroarm copolymers were modeled on the basis of the μ-EOF copolymers used in the experiments performed by Lodge and co-workers [189]. Their simulations demonstrated that the length of the solvent-philic block has a significant effect on the shape of the multicompartment micelles formed from ABC heteroarm copolymers. They found that the more discrete micelles can be formed when the solvent-philic blocks are longer, and the worm-like micelles can be observed when the solvent-philic blocks are shorter. Similar results were obtained in analytical scaling predictions proposed by Zhulina and co-workers [191]. A more systematic study of the self-assembly of ABC heteroarm copolymers in solution has been carried out by Kong et al. through lattice Monte Carlo simulations [192]. By varying the block compositions of different arms, a variety of microstructures including hamburger micelles (HM), segmented bilayers (SB), segmented semivesicles (SSV), laterally structured vesicles (LSV), laterally structured micelles (LSM), raspberry micelles (RM), multicompartment worms (MW) and multicompartment onions (MO) were observed, as shown in Fig. 17. They demonstrated that the overall micelle shape strongly depends on the block composition of solvent-philic A arms f_A, and the internal segregated microstructures rely on the ratio between the block compositions of the two solvent-phobic arms. These novel micel-

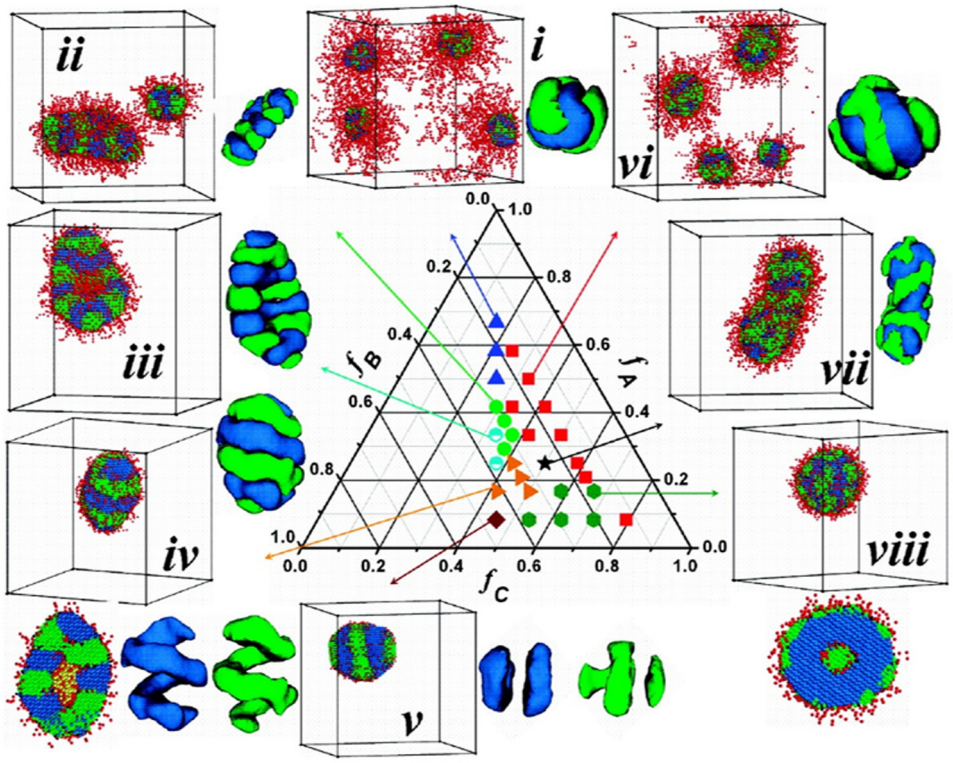

Fig. 17. Morphological phase diagram of the ABC heteroarm copolymers as functions of the block compositions of the A, B and C arms (f_A, f_B and f_C). The red, green and blue colors are assigned to the solvent-philic A arms, the solvent-phobic B arms and the solvent-phobic C arms, respectively. [192], Copyright 2009. (For interpretation of the references to colour in this figure legend, the reader is referred to the web version of this article.)

Reproduced with permission from the American Chemical Society.

lar structures have been confirmed by Wang et al. through EPD simulations [193]. In their simulations, the thermodynamic stability of vesicles with alternating ring-shape strings was examined by the combination of the Helfrich's membrane model and the strong segregation theory of block copolymers. Furthermore, Wang et al. investigated the formation pathway of the multicompartment vesicles formed from ABC heteroarm copolymers. They demonstrated that, when the block composition of the solvent-phobic arms is small, only few solvent-phobic nuclei can be formed in the initial stage of self-assembly. In this case, two steps including nucleation and growth were observed during the formation of multicompartment vesicles. While with increasing the block composition of the solvent-phobic arms, the number of solvent-phobic nuclei increases and three steps including nucleation, coalescence and growth have been found during the formation of the multicompartment vesicles. Their simulations indicate that the number of the solvent-phobic nuclei in the initial stage has a significant influence on the formation pathway of the multicompartment vesicles.

5.2. Dendritic copolymers

Dendritic copolymers, including dendrimers and hyperbranched copolymers, are copolymers with three-dimensional highly branched architecture. The dendritic copolymers have shown great advantages of numerous functional groups, low entanglement and solution viscosity behavior [194–196]. These superior properties of the dendritic copolymers strongly rely on their intramolecular conformation and intermolecular self-assembly behaviors. There was an assumption that the segmental density of dendritic copolymers in solution increases from the center to the periphery [197]. Lescanec and Muthukumar firstly proposed a dense core description of the dendritic copolymers by a theoretical simulation [198]. In their simulations, a self-avoiding walk algorithm has been employed to simulate the dendritic molecules. Their simulations have gained a great of support from SANS and SAXS investigations. In spite of the progress made in theoretical simulations of the intramolecular conformation of dendritic copolymers, the simulation investigation about the intermolecular self-assembly of dendritic copolymers is still scarce.

Recently, large micelles with diameters exceed 100 nm, that have proved to be multimicelle aggregates (MMA) formed by interconnection of small micelles [199], were prepared through the self-assembly of dendritic copolymers in solution. The simulation investigations about the MMA structures formed from dendritic copolymers have been carried out by Yan et al. through DPD method [200,201]. In their simulations, the coarse-grained models of dendrimers and hyperbranched copolymers with solvent-phobic A cores and solvent-philic B arms were constructed according to the experimental density. Their investigations reported two kinds of mechanisms for the formation of MMA, that have been defined as the unimolecular micelle aggregate (UMA) mechanism (Fig. 18(a)) and the small micelle aggregate (SMA) mechanism (Fig. 18(b)). They found that these two mechanisms strongly depend on the solvent-phobicity of the cores and the solvent-philicity of the arms. Furthermore, with increasing the degree of branching, the structural transitions of the assemblies from spherical micelles to worm-like micelles and then to vesicles have been observed. Their simulations provide useful details that are difficult to be captured in experiments.

The dendritic copolymers with asymmetric architectures, that can act as amphiphiles with greater versatility than simple diblock copolymers and symmetric dendritic copolymers, have drawn a lot of attention [202,203]. One type of the asymmetric dendritic copolymers is the Janus dendrimers consisting of two chemically distinct dendritic blocks [204]. Using coarse-grained MD method, Percec et al. studied the self-assembly behaviors of Janus

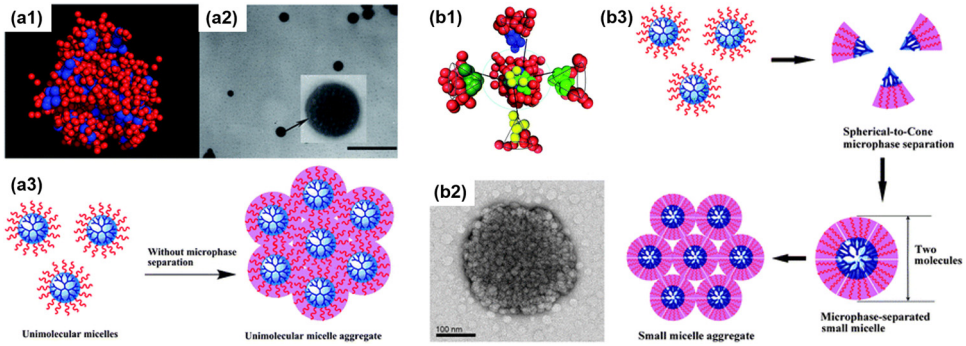

Fig. 18. (a) The UMA mechanism of the multimolecular micelles: (a1) a magnified multimolecular micelle, the hydrophobic dendritic core is represented by blue beads, the hydrophilic linear arms are represented by red beads; (a2) typical TEM image of the UMA micelles (the scale bar represents 400 nm); (a3) the schematic for UMA mechanism. (b) The SMA mechanism of the multimolecular micelles: (b1) the cross-sectional view of the small micelle, the hydrophobic dendritic core is represented by blue, light green and yellow beads, the hydrophilic linear arms are represented by red beads; (b2) typical TEM image of SMA micelles (the scale bar represents 100 nm); (b3) the schematic for SMA mechanism. [200], Copyright 2009. (For interpretation of the references to colour in this figure legend, the reader is referred to the web version of this article.)

Reproduced with permission from the Royal Society of Chemistry.

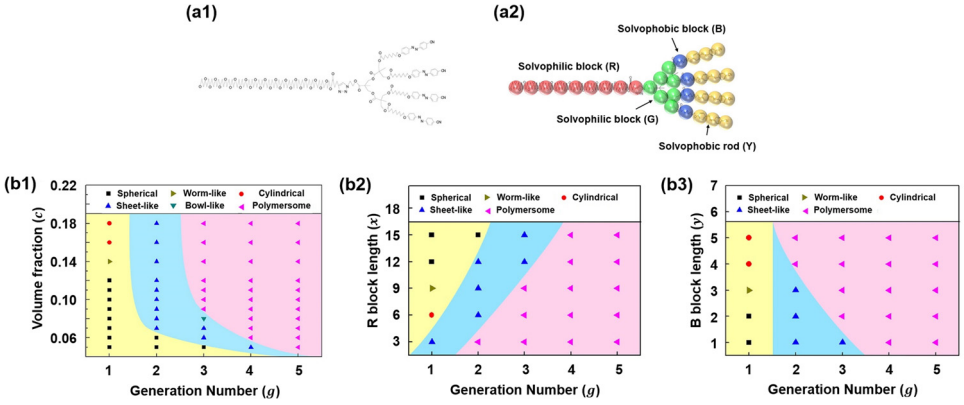

Fig. 19. (a) Schematic diagrams of (a1) the realistic linear-dendritic block copolymer PEG_{27}-*dendr*$[AZO]_4$ and (a2) its coarse-grained model R_x-*dendr*$[B_y\text{-}Y_3]_4$. This linear-dendritic block copolymer is with two generations ($g = 2$) and thus has four azobenzene mesogens ($n = 4$). (b) Morphological phase diagrams of the linear-dendritic copolymer systems: (b1) morphological phase diagram of R_{12}-*dendr*$[B_2\text{-}Y_3]_4$; (b2) morphological phase diagram of R_x-*dendr*$[B_2\text{-}Y_3]_4$; (b3) morphological phase diagram of R_{12}-*dendr*$[B_y\text{-}Y_3]_4$. [206], Copyright 2012.

Reproduced with permission from the American Chemical Society.

dendrimers in solution [205]. In their simulations, different models of Janus dendrimers have been constructed based on their experiments, and the coarse-grained interaction potentials were derived by the all-atom simulations. Combining the coarse-grained MD smulations with experiments, various self-assembled structures including bilayers, vesicles, disk-like micelles and toroidal micelles have been investigated. However, the influence of the molecular parameters on the self-assembly of asymmetric dendritic copolymers has not been explained in their simulations. In a recent work, Lin et al. employed DPD method to investigate the self-assembly of another kind of asymmetric dendritic copolymers, *i.e.*, linear-dendritic block copolymers [206]. To simulate the azobenzene-containing (AZO) linear-dendritic block copolymers PEG_{27}-*dendr*$[AZO]_4$ synthesized by del Barrio et al. [202], they constructed a coarse-grained model of R_x-*dendr*$[B_y\text{-}Y_3]_4$ in which an spring force is introduced to simulate the rod-like azobenzene, as shown in Fig. 19(a). A variety of self-assembled structures including spherical micelles, worm-like micelles, cylindrical micelles, hamburger-like micelles, sheet-like micelles, bowl-like micelles and vesicles were observed. The influence of the molecular architecture and the volumetric fraction of copolymers on the self-assembled structures formed from R_x-*dendr*$[B_y\text{-}Y_3]_4$ copolymers was examined systematically, and a series of morphological phase diagrams have been obtained, as displayed in Fig. 19(b). They further studied the effect of ultraviolet irradiation on the morphology of the vesicular structures through changing the solvent-philicity of Y blocks. Their simulations are in good agreement with the experiments carried out by del Barrio and co-workers [202].

Although some progress in the area of the self-assembly of dendritic copolymer solutions has been achieved through theoretical simulations, further development of simulation technique is still required to investigate the self-assembly of dendritic copolymers. For instance, due to the large computational cost in the simulations of the dendritic copolymers, the computational efficiency of simulations needs to be improved. The developments of corresponding parallel algorithms provide a promising way to enhance the computational efficiency. In addition, the simulation of the large compound vesicle formed from dendritic copolymers is absent because the assembly dimension (10–100 μm) excesses the computing capability [207]. The multiscale modeling and simulation techniques offer an opportunity to overcome this obstacle.

5.3. Bottle-brush copolymers

Bottle-brush copolymers, also called copolymer brushes, are highly-branched macromolecules consisting of a linear backbone and densely grafted side chains [180,208–210]. As a type of natural bottle-brush copolymers comprising a protein backbone and carbohydrate side chains, proteoglycans have been found in different places in human body performing significant functions. For

instance, proteoglycans have been performed to play significant roles in controlling the shock absorption and lubrication properties in cartilage [211,212]. The biological significance of natural bottle-brush copolymers inspires polymer scientists to synthesize the bottle-brush copolymers and investigate their self-assembly behaviors in solution. Several theoretical simulation methods including MC [213–215], MD [216,217], DPD [218] and SCFT [219] have been employed to study the self-assembly behaviors of the bottle-brush copolymers. Using MC and MD methods, a series of simulations of the intramolecular self-assembly of the bottle-brush copolymers comprising two types of side chains have been carried out by Binder and co-workers [213–217]. The structural transition from the "pearl-necklace" assemblies to dense cylinders has been observed by varying the solvent selectivity and the grafting density. And the "Janus dumbbell" assemblies have been observed when the grafting density is large. They demonstrated that these structural transitions occur gradually and no sharp structural transitions as found in block copolymer melts take place due to the quasi-1D characteristic of the bottle-brush copolymers.

The molecular asymmetry of the bottle-brush copolymers has a profound influence on their self-assembly behaviors. Through SCFT method, Wang et al. calculated the free energy of the micellar structures formed from the asymmetric bottle-brush copolymers A-*b*-(A-*g*-B) in B-selective solvents [219]. In their SCFT calculations, the free energy of the micellar system exhibits two minima, indicating the existence of the bimodal distribution of micelles. By examining the density profiles of the micelles, they found that the bimodal distribution of micelles is the result of the separation inside the comb blocks and the separation between the coil blocks and the comb blocks. In a recent work, Chang et al. utilized DPD method to study the multilayered vesicles formed from amphiphilic asymmetric bottle-brush copolymers [218]. In their DPD simulations, the CG models of Y_{15}-*g*-(R_x/B_y-*b*-G_z) copolymers have been constructed to mimic the PGMA-*g*-(PEO/PS-*b*-PNIPAM) bottle-brush copolymers in the experiments carried out by Lian and co-workers [220], as shown in Fig. 20(a). They found that, consistent with the experimental observations, the Y_{15}-*g*-(R_x/B_y-*b*-G_z) copolymers can self-assemble into multilayered asymmetric vesicles. Except for the multilayered vesicles observed in experiments, several micellar structures have been found by adjusting the length of solvent-philic blocks in the diblock side chains B_y-*b*-G_z, as illustrated in Fig. 20(b). They concluded that, similar to the linear copolymers, a structural transition from vesicles to micelles can take place as the increase of the length of solvent-philic blocks. They further investigated the influence of the grafting density on the self-assembled structures formed from Y_{15}-*g*-(R_1/B_7-*b*-G_2) copolymers. By increasing the grafting density, the structural transitions from hamburger micelles to vesicles then to donut micelles have been observed. Their simulations provide an example for qualitatively simulating the self-assembly of the bottle-brush copolymers in solution by mesoscopic method.

The above-cited simulation studies have proven that the theoretical simulation techniques are powerful tools to study the intramolecular and intermolecular self-assembly of the bottle-brush copolymers in solution. Both the results of the field-theoretical method and the particle-based method have successfully reproduced the results in experiments. However, the simulation studies of the self-assembly of the bottle-brush copolymers are still at an exploratory stage. To realize the potential applications of the bottle-brush copolymers, a more profound understanding of the self-assembly kinetics, the structural stability and the structure-property relation is required. For example, the understanding of the formation kinetics of the bottle-brush copolymer assemblies and their cellular endocytosis processes can be helpful for realizing the potential biomedical applications. There is no doubt that the theoretical simulation can offer a promising way to tackle these problems.

6. Self-assembly of mixture systems

Despite the great progress achieved in the field of self-assembly of copolymers in solution, it is still a challenge to prepare the desired microstructures through the self-assembly of single component polymer systems in solution. The mixture systems comprising two or more components provide another promising route to create novel and functional materials. For example, Lodge and co-workers demonstrated that the "hamburger" micelles can be formed from the binary mixture of poly(ethylethylene-*b*-ethylene oxide) (PEE-*b*-PEO) diblock copolymers and μ-EOF star-like terpolymers in solution [221], and Voets et al. prepared disk-shaped Janus micelles from a mixture of poly(acrylic acid-*b*-acryl amide) (PAA-*b*-PAAm) and poly(2-methylvinylpyridinium iodide-*b*-ethylene oxide) (P2MVP-*b*-PEO) in aqueous solution [222]. However, the diversity of polymer components brings the difficulty to analyze the self-assembled structures experimentally, and the investigations of the thermodynamic stability and the formation pathway of the self-assembled structures in polymer mixture systems exceed the capability of experimental techniques. In this regard, theoretical simulations offer an effective way to investigate the self-assembly behaviors of polymer mixtures in solution. In this section, we focus on the simulations about the self-assembly of polymer/polymer mixtures and polymer/nanoparticle mixtures in solution.

6.1. Polymer/polymer mixtures

For the self-assembly of polymer/polymer mixtures in solution, an important issue is whether the co-assembly of polymer/polymer mixtures can take place or not. Palyulin et al. developed a theoretical framework to study the mixture of AB and BC diblock copolymers in solvents selective for A and C blocks [223]. In their theoretical calculations, the thermodynamic stability of different micellar structures was analyzed and a morphological phase diagram of the AB/BC mixtures in solution was constructed. They demonstrated that the micelles with A and C blocks homogeneously mixed within the corona are thermodynamic stable when the incompatibility between A and C blocks is weak. Compared with theoretical analysis, computer simulation is a more straightforward way to study the self-assembly behaviors of polymer/polymer mixtures in solution. Employing three-dimensional SCFT method, Lin et al. systematically studied the self-assembly behaviors of the mixture of AB and BC diblock copolymers in dilute solution with solvent-phobic A blocks [224]. In their simulations, two cases have been studied: in one case the block compositions of solvent-phobic A blocks in AB copolymers and AC copolymers are equal, and in the other one the block composition of solvent-phobic A block in AB copolymers is smaller than that in AC copolymers. A variety of aggregates such as spherical micelles (M), cylindrical micelles (C), quasi-vesicles (QV) and vesicles (V) have been observed in both cases. The morphological phase diagrams in the two cases have been constructed, as shown in Fig. 21 (a). The structural transitions observed in their simulations are in qualitative agreement with some experimental observations [225]. Furthermore, they studied the chain segregation in vesicles and micelles by calculating the density distributions of different blocks, and a structural transition mechanism induced by chain segregation has been proposed.

In addition to the binary mixture of diblock copolymers in solution, the theoretical simulations have also been used to study the self-assembly of mixture systems containing copolymers with different architectures. Ma et al. employed SCFT method to investigate

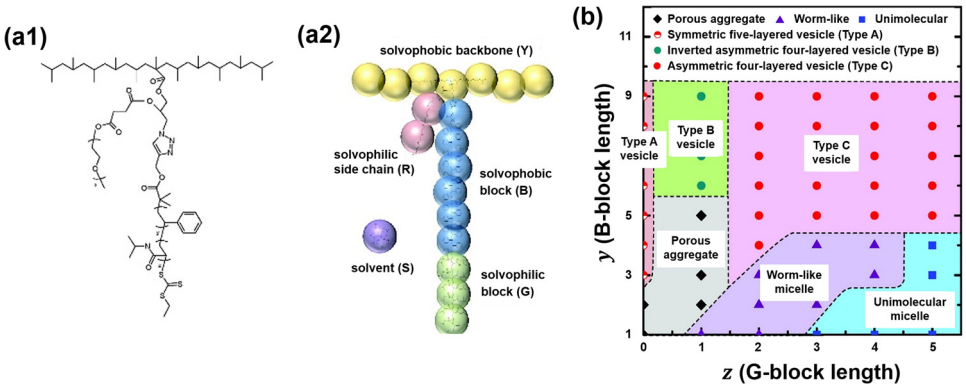

Fig. 20. (a) Schematic diagrams of (a1) the bottle-brush copolymer PGMA-*g*-(PEO/PS-*b*-PNIPAM) and (a2) its coarse-grained model Y_{15}-*g*-(R_x/B_y-*b*-G_z). (b) Morphological phase diagrams of the assemblies formed from Y_{15}-*g*-(R_1/B_y-*b*-G_z) copolymers as functions of the length of B blocks *y* and the length of G blocks *z*. [220], Copyright 2012. Reproduced with permission from the American Chemical Society.

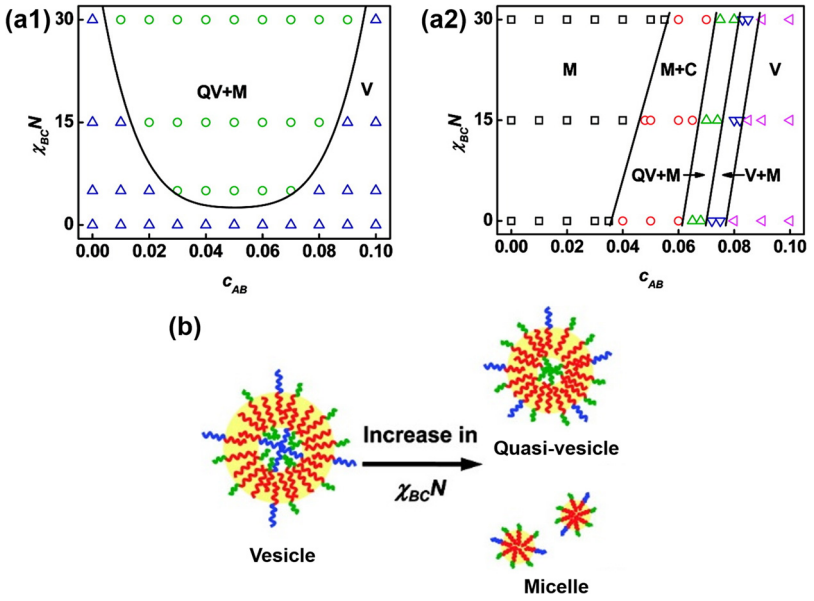

Fig. 21. (a) Morphological phase diagrams of the AB/AC mixtures in solution as functions of the Flory-Huggins interaction strength $\chi_{BC}N$ and the volumetric fraction of AB diblock copolymers c_{AB}: (a1) the block compositions of solvent-philic A blocks in copolymers AB and AC are equal; (a2) the block composition of solvent-philic A block in AB copolymers is smaller than that in AC copolymers. (b) Schematic of the structural transition from vesicles to quasi-vesicles and spherical micelles. [224], Copyright 2009. Reproduced with permission from the American Chemical Society.

the self-assembly of the mixture of the ABC star-like copolymers and the AB diblock copolymers with solvent-philic A blocks and solvent-phobic B and C blocks [226]. In their calculations, the structural transitions observed in the experiments carried out by Lodge et al. have been successfully reproduced [221]. However, the mechanism underlying these structural transitions has not been discussed in their investigations. In a recent work, Lin et al. used SCFT to investigate the mechanism underlying the structural transitions observed in their experiments of the self-assembly of vesicle-forming graft and block copolymer mixtures in solution [227]. In their simulations, the interesting feature that the vesicle-forming PBLG-*g*-PEG and PBLG-*b*-PEG copolymers cooperatively assemble into cylindrical micelles instead of vesicles was captured, and the detailed information of chain distributions in the micellar aggregates was analyzed. They found that the ends of cylindrical micelle are capped by the solvent-philic blocks of block copolymers, whereas the body of cylindrical micelle is covered by the solvent-philic blocks of graft copolymers. Their simulations provide direct interpretation of the co-assembly of copolymer mixtures in solution.

The introducing of chain rigidity in the mixture of polymers can lead to complex self-assembled structures, that also can be taken into consideration through simulation techniques. Using DPD method, Lin et al. studied the self-assembly behaviors of the mixture of coil-rod graft copolymers and rigid homopolymers in solution [228]. In their simulations, the coarse grained models of coil-rod graft copolymer and rigid homopolymer are constructed on the basis of the poly(acrylic acid-*g*-γ-benzyl-L-glutamate)/poly(γ-benzyl-L-glutamate) (PAA-*g*-PBLG/PBLG) mixtures, and the rigidity of the rod blocks is realized by the angle potential between every two consecutive bonds. The formation of toroidal micelles observed in experiments has been successfully reproduced in their DPD simulations. Furthermore, they found that the toroidal micelles are formed through the end-to-end connection of curved rods and the rigid homopolymers self-assemble into the interior cores of aggregates.

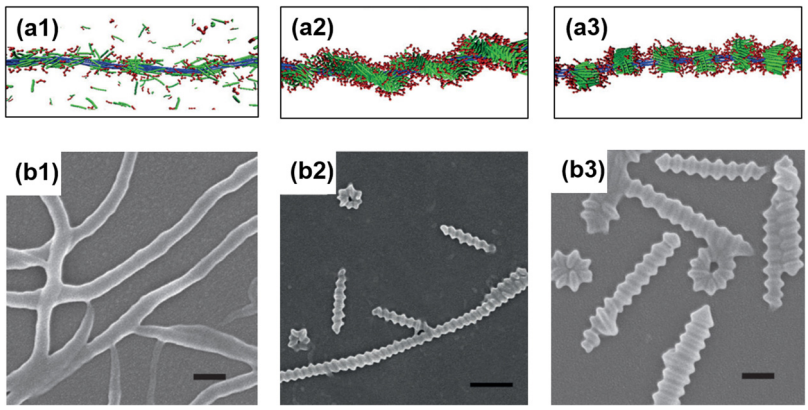

Fig. 22. (a) Simulation results for the hierarchical structures self-assembled from the mixture of A_7B_3 rod-coil block copolymers and A_{150} rigid homopolymers in solution: (a1) plain fiber structure with high A–A interactions of $\varepsilon_{AA} = 2.4$; (a2) superhelices with moderate A–A interactions of $\varepsilon_{AA} = 2.1$; (a3) abacus-like structures with low A–A interactions of $\varepsilon_{AA} = 1.6$. (b) SEM images of aggregates self-assembled from the PBLG-*b*-PEG/PBLG mixtures at various temperatures: (b1) plain fibers formed at 5 °C; (b2) superhelices formed at 20 °C; (b3) abacus-like structures formed at 40 °C. Scale bars: (b1 and b3) 200 nm, (b2) 500 nm. [229], Copyright 2013.
Reproduced with permission from the John Wiley & Sons Inc.

Recently, Lin et al. performed BD simulations on the self-assembly of the mixture of rod-coil (or coil-coil) block copolymers and rigid (or flexible) homopolymers in solution [229]. By adjusting a series of parameters, including the association strength between different blocks, the segment rigidity and the volumetric fractions of the two components, the structural transitions from abacus-like (beads-on-wire) structures to superhelices and then to plain fibers have been observed, as presented in Fig. 22(a). According to their simulations, they synthesized an array of block copolymers (*e.g.*, PBLG-*b*-PEG and PS-*b*-PEG) and homopolymers (*e.g.*, PBLG and PS) to study the effect of temperature, that corresponds to the association strength between the rod blocks of copolymers and the rigid homopolymers in their simulations, on the self-assembly of the copolymer/homopolymer mixtures in solution. The superhelices and abacus-like structures predicted by simulations have been confirmed in their experiments, as shown in Fig. 22(b). And the chain distribution information provided by simulations suggested that the superhelical structures observed in experiments consist of large-length-scale inner bundles formed from solvent-phobic PBLG homopolymers and small-length-scale helical strings formed from PBLG-*b*-PEG block copolymers. In a subsequent work [230], the structural stability regions of the rod-coil block copolymer/rigid homopolymer mixtures as functions of the lengths of rod and coil blocks were mapped. And two levels of rod block ordering, including the helical strings formed from block copolymers wrapping on the homopolymer bundles and the twisting packing of the rod blocks inside the strings, existing in the superhelical structures was found. These pioneering works imply that the combination of simulation and experiments is an effective strategy for the investigation of polymeric self-assembly.

6.2. Polymer/nanoparticle mixtures

The encapsulation of nanoparticles into copolymer assemblies provides a promising route to prepare novel materials with enhanced mechanical, optical, electric and magnetic properties [231–234]. The realization of these advanced properties requires precise control on the morphology of copolymer assemblies and the location of nanoparticles, both of that are determined by the enthalpic and entropic interplays within the system. The enthalpic and entropic interplays can be influenced by a variety of factors, such as the compatibility between copolymers and nanoparticles, the ratio of the size of nanoparticles to the gyration radius of copolymers, the rigidity of copolymer chains and the shape of nanoparticles. An exhaustive discussion about these issues at a nanoscale remains a challenging task in experimental studies. Recently, several simulation methods have been successfully applied to study the self-assembly of the mixture of polymers and nanoparticles in solution [235–238]. These simulations mainly concerned two aspects: the location of nanoparticles in copolymer assemblies and the structural transition of copolymer assemblies induced by nanoparticles. In this subsection, simulations about these two aspects are reviewed, and some novel modeling and simulation techniques developed to investigate the self-assembly of polymer/nanoparticle mixtures are introduced.

The SCFT method has been successfully applied to investigate the thermodynamic properties of copolymers in the absence of nanoparticles both in bulk and in solution. By coupling the SCFT method for polymers with the DFT method for nanoparticles, Balazs et al. developed a numerical approach to study the self-assembly of the mixture of polymers and nanoparticles in bulk [239]. The variation of enthalpy and entropy underlying the self-assembly of the polymer/nanoparticle mixtures can be analyzed by their method. Zhang et al. firstly extended this method to study the self-assembly behaviors of AB diblock copolymer/nanoparticle mixtures in solution [240]. In their simulations, both A-selective and nonselective solvent-phobic nanoparticles were considered. They systematically investigated the influences of the volumetric fraction of nanoparticles c_P and the radius of nanoparticles R_P on the self-assembly behaviors of the diblock copolymer/nanoparticle mixtures in solution. For the A-selective solvent-phobic nanoparticles, a structural transition from vesicles to spherical micelles (S) and cylindrical micelles (C) with increasing the radius or the volumetric fraction of nanoparticles has been observed; while for the nonselective solvent-phobic nanoparticles, the vesicles were replaced by the large compound micelles (LCM), and the spherical micelles emerged as the increase of the radius or the volumetric fraction of nanoparticles. The morphological phase diagrams as functions of the radius and the volumetric fraction of nanoparticles have been constructed, as shown in Fig. 23(a). Pan et al. extended this SCFT/DFT approach to study the self-assembly of bi-disperse nanoparticles/diblock copolymer mixtures in solution [235]. The influences of the chemical incompatibility between different nanoparticles and the steric packing interactions among nanoparticles on the self-assembled structures have been investigated. By calculating the enthalpy and the entropy of the mixtures, they found that the separation of nanoparticles with different radii is driven by the variation of the entropy. Furthermore, they found that an increase of the chemical incompatibility between different nanoparticles can induce the formation of “a jujube set in a cake”

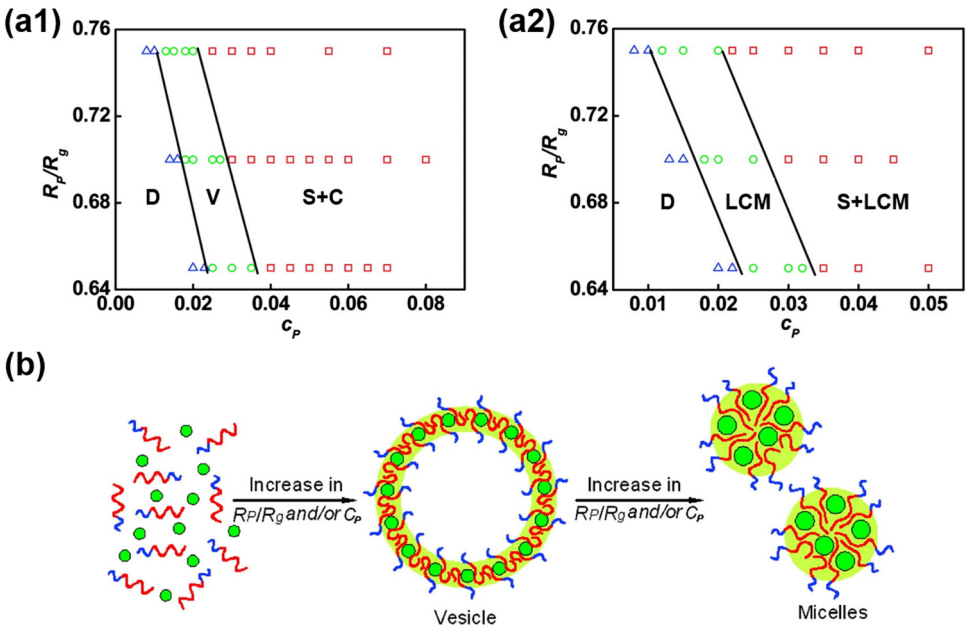

Fig. 23. (a) Morphological phase diagrams of the AB diblock copolymer/nanoparticle mixtures with (a1) A-selective solvent-phobic nanoparticles and (a2) nonselective solvent-phobic nanoparticles plotted as functions of the radius R_P/R_g and the volumetric fraction c_P of nanoparticles. (b) Schematic of the structural transitions from disorder state to vesicles and then micelles for the AB diblock copolymer/nanoparticle mixtures in solution. [240], Copyright 2007.
Reproduced with permission from the American Chemical Society.

hierarchical structure, that provides a route to fabricate complex microstructures through diblock copolymer/nanoparticle mixture systems.

Although the SCFT/DFT approach has proven to be effective for investigating the polymer/nanoparticle mixtures, it is difficult to be applied to systems in which the reliable density functional is inavailable. To solve these problems, Fredrickson and co-workers developed a hybrid modeling and simulation technique named HPF method [64]. In the theoretical framework of the HPF method, the copolymers are described in the field-theoretic context but not restricted to the mean-field approximation. The coordinates of nanoparticles are explicitly retained and the configurations of nanoparticles are sampled through Brownian dynamic strategy or force-bias MC scheme, different from the SCFT/DFT approach. Ma et al. extended the HPF method to study the self-assembly behaviors of AB diblock copolymer/nanoparticle mixtures in solution [236]. They found that the surface selectivity of nanoparticles is a key factor to control the location of nanoparticles in the assemblies formed from AB diblock copolymers. The influence of the volumetric fraction of nanoparticles on the self-assembled structures was investigated, as shown in Fig. 24. The structural transitions from vesicles to cylindrical micelles and then to spherical micelles with increasing the volumetric fraction of nanoparticles was observed, in agreement with the results reported by Zhang and co-workers [240].

The above simulations improve our understanding of the self-assembly of the mixture of nanoparticles and flexible copolymers in solution. However, the self-assembly of the mixture of nanoparticles and rigid copolymers in solution has been seldom studied. Compared with the flexible copolymers, the copolymers containing rigid blocks exhibit distinct self-assembly behaviors due to the ordered packing of rigid blocks. Thus, it is expected that the addition of nanoparticles would destroy the ordered packing of rigid blocks and then deform the self-assembled structures. To demonstrate this issue, Lin et al. employed DPD simulations to study the structural transition of PBLG-*b*-PEG aggregates induced by the addition of Au nanoparticles observed in experiments [238]. In their simulations, the CG model in which the PBLG-*b*-PEG block copolymers are modeled as rod-coil block copolymers and the Au nanoparticles are modeled as single beads has been constructed. Through analyzing the order parameter of rod blocks, they found that the encapsulation of nanoparticles in the micellar structures leads to the breakage of the ordered packing of PBLG rods and causes a structural transition from cylindrical micelles to spherical micelles, in qualitative agreement with their experimental observations. Furthermore, their simulations suggested that the nanoparticles tend to locate near the core/shell interface and in the core center of the aggregates. Their simulations help us understand the self-assembly behaviors of such mixture systems.

While the self-assembly of polymer/nanoparticle mixtures in solution has been effectively studied through simulation techniques, further explorations about these systems are still needed. One of the significant issues in this field is the mixture systems containing anisotropic nanoparticles. For example, the experimental studies have demonstrated that the location and orientation of gold nanorods can be tuned in cylindrically microdomains of block copolymer-based supramolecular assemblies [241]. And the transition of the configurations of nanorods from end-to-end organization to side-by-side arrangement provides a possible way to control the plasmonic properties of nanorods. However, the simulation investigations in this field are still in absence. Several simulation techniques including DPD method and HPF technique are suggested to be suitable to study this topic straightforwardly.

7. Conclusion remarks and outlook

In the past decades, the self-assembly of copolymers in solution has been a subject of great interest due to its promising applications in many fields. The simulation techniques including particle-based, field-theoretic and hybrid modeling methods have effectively assisted the experimentalists to make a further step in understanding the self-assembly of copolymer solutions. In this

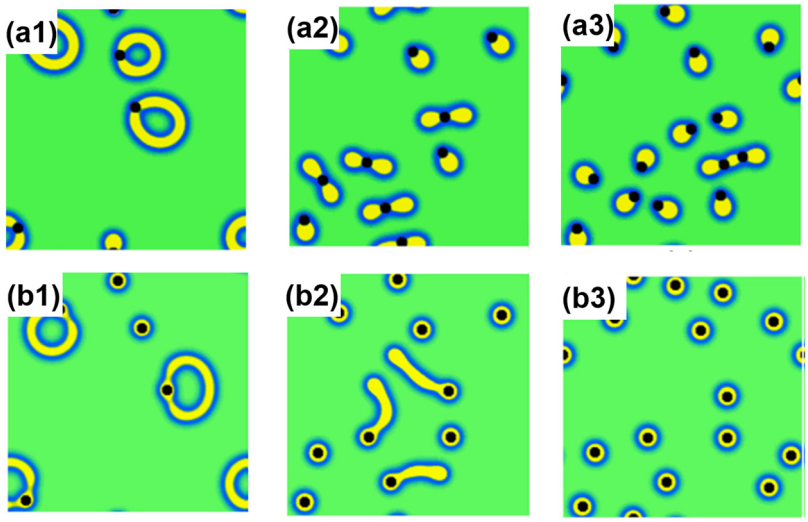

Fig. 24. The equilibrium morphologies of AB diblock copolymer/nanoparticle mixtures as a function of the number of nanoparticles N_P. (a) Solvent-philic nanoparticles: (a1) $N_P = 5$; (a2) $N_P = 10$; (a3) $N_P = 15$. (b) Solvent-phobic nanoparticles: (b1) $N_P = 5$; (b2) $N_P = 10$; (b3) $N_P = 15$. The yellow, blue, green and black colors are assigned to solvent-phobic A blocks, solvent-philic B blocks, solvents and nanoparticles, respectively. [236], Copyright 2011. (For interpretation of the references to colour in this figure legend, the reader is referred to the web version of this article.)

Reproduced with permission from the Elsevier Science Ltd.

review, the simulation investigations about the self-assembly of the linear block copolymers, the graft copolymers, the star-shaped copolymers, the dendritic copolymers, the bottle-brush copolymers and the polymer mixtures in solution have been featured. The studies reviewed here suggest that the self-assembled structures formed from copolymers in solution are dominated by the complicated interplay between the enthalpy and the entropy, that can be tuned by several molecular parameters such as the solvent-philicity and the block rigidity of polymers. In addition, by grafting the branched arms onto the linear backbone or introducing the second component into polymer system, various assemblies with hierarchical nanostructures can be formed. Furthermore, these studies suggest that the formation kinetics also has an important influence on the self-assembled structures. Despite the great development that has been made in the field of theoretical modeling and simulation about the self-assembly of polymers in solution, there are still many challenges, that are also opportunities, guiding the future directions in this field.

- *The rules underlying hierarchical self-assembly*. Inspired by the nature, hierarchical self-assembly involving more than two levels of self-assembly steps or orders has been considered as a hopeful "bottom-up" strategy for the preparation of novel functional materials [242–244]. In particular, the hierarchical self-assembly of copolymers in solution provides a way to produce assemblies with specified morphology and monodispersed size. For example, a precise control over the superstructures formed from linear ABC triblock copolymers in solution through hierarchical self-assembly strategy has been reported by Gröschel and co-workers [166]. Nevertheless, the rules dominating the hierarchical self-assembly of copolymers in solution, especially how to choose the pathway escaping from undesirable metastable states and how to control the formation kinetics of the hierarchical assemblies, still remain vague. Fortunately, the theoretical simulations not only can help us plot the free energy landscape of polymer systems but also is able to gain insights into the kinetics of the hierarchical self-assembly.
- *The relation between the microstructure of polymer assemblies and their functional properties*. It is well acknowledged that the macroscopic properties of polymer assemblies are dominated by the molecular groups of macromolecules and their mesoscopic morphologies. For example, the micelles self-assembled from polymers with optical function groups exhibit multifarious optical properties [245,246]. In another potential application of polymer micelle as drug carrier, the drug encapsulation ability of the micelle-based drug carrier has a strong dependence on its geometrical characteristic [247–249], that can be tuned through the self-assembly of polymers. Although the knowledge of the self-assembled structures formed from polymers in solution has already been enriched to some extent, the correlation between the nano and mesoscopic details of assemblies and their macroscopic properties is still a field less explored. The investigations of the structure-property relation of polymer assemblies require a further development of the modeling and simulation techniques. Multiscale modeling approach capturing processes at all relevant length scales could be a promising strategy to achieve this goal. And hybrid modeling method combining methods with different length scales may provide another choice. For both of them, a framework for mapping atomistic configurations to coarse-grained models is required.
- *The "synergistic interaction" between simulations and experiments*. In the field of polymer science, the combination of experiments and simulations is of great importance. On one side, the correction of the simulation models based on the specific experimental systems is necessary to acquire the formed structures and the related formation kinetics as accurately as possible. On the other hand, simulations can provide an in-depth understanding about the experimental observations and the directions for future experiments. A "synergistic interaction" between simulations and experiments can effectively promote the fabrication of advanced functional materials. For example, with the help of SCFT simulations, the mechanism underlying the structural transition observed in PBLG-*g*-PEG/PBLG-*b*-PEG mixtures in solution has been investigated by Lin and co-workers [227]. In another example, the BD method assists Lin et al. to prepare supramolecular structures including superhelices and abacus-like structures through the self-assembly of polypeptide-based copolymers in solution [229,230]. To realize the "synergistic

interaction" between simulations and experiments, the construction or improvement of simulation models to characterize the experimental conditions precisely is of primary importance.

- *Large scale simulation by parallel algorithm acceleration*. The finite size effect [250] is a ubiquitous problem in simulations. For instance, Wang et al. found that the multilamellar vesicular structures are more stable in a larger simulation box [137]. This problem can be alleviated by enlarging the size of simulation box, that means an unaffordable computing cost in the past. Accelerating the simulations by parallel algorithm is a promising way to operate large-scale simulations. GPU is an innovative video card that can be used not only to show graphics but also for scientific calculations [251]. With the assistance of the parallel computing architectures including Compute Unified Device Architecture (CUDA) and Open Computing Language (OpenCL), the processing power of GPU can be harnessed. Specially, the GPU technology proves to be a particularly good fit for the particle-based method due to the massively parallel nature shared by the evaluation of inter-particle force. To take full advantage of the computing power of GPU, the efficient parallel algorithms for existing simulation methods should be developed in coming years.

Acknowledgements

This work was supported by the National Natural Science Foundation of China (21234002, and 21474029). Support from Projects of Shanghai municipality (16520721900, 14DZ2261205) is also appreciated.

References

[1] Bishop KJ, Wilmer CE, Soh S, Grzybowski BA. Nanoscale forces and their uses in self-assembly. Small 2009;5:1600–30.
[2] Mai Y, Eisenberg A. Self-assembly of block copolymers. Chem Soc Rev 2012;41:5969–85.
[3] Discher DE, Eisenberg A. Polymer vesicles. Science 2002;297:967–73.
[4] Bae Y, Fukushima S, Harada A, Kataoka K. Design of environment-sensitive supramolecular assemblies for intracellular drug delivery: polymeric micelles that are responsive to intracellular pH change. Angew Chem Int Ed 2003;42:4640–3.
[5] Chen Q, Schönherr H, Vancso GJ. Block-copolymer vesicles as nanoreactors for enzymatic reactions. Small 2009;5:1436–45.
[6] Xu Z, Lin J, Zhang Q, Wang L, Tian X. Theoretical simulations of nanostructures self-assembled from copolymer systems. Polym Chem 2016;7:3783–811.
[7] Schatz GC. Using theory and computation to model nanoscale properties. Proc Nat Acad Sci USA 2007;104:6885–92.
[8] Allen MP, Tildesley DJ. Computer simulation of liquids. Oxford: Oxford University Press; 1989, 408 pp.
[9] Frenkel D, Smit B. Understanding molecular simulation: from algorithms to applications. San Diego: Academic Press; 2001, 664 pp.
[10] Rapaport DC. The art of molecular dynamics simulation. Cambridge: Cambridge University Press; 2004, 564 pp.
[11] Zeng QH, Yu AB, Lu GQ. Multiscale modeling and simulation of polymer nanocomposites. Prog Polym Sci 2008;33:191–269.
[12] Glotzer SC, Paul W. Molecular and mesoscale simulation methods for polymer materials. Annu Rev Mater Res 2002;32:401–36.
[13] Di Marino D, Bonome EL, Tramontano A, Chinappi M. All-atom molecular dynamics simulation of protein translocation through an α-hemolysin nanopore. J Phys Chem Lett 2015;6:2963–8.
[14] Merz Jr KM, Ferguson DM, Spellmeyer DC, Fox T, Caldwell JW, Kollman PA. A second generation force field for the simulation of proteins, nucleic acids, and organic molecules. J Am Chem Soc 1995;117:5179–97.
[15] MacKerell Jr AD, Bashford D, Bellott M, Dunbrack Jr RL, Evanseck JD, Field MJ, et al. All-atom empirical potential for molecular modeling and dynamics studies of proteins. J Phys Chem B 1998;102:3586–616.
[16] Simmerling C, Strockbine B, Roitberg AE. All-atom structure prediction and folding simulations of a stable protein. J Am Chem Soc 2002;124:11258–9.
[17] Klein ML, Shinoda W. Large-scale molecular dynamics simulations of self-assembling systems. Science 2008;321:798–800.
[18] Shaw DE, Maragakis P, Lindorff-Larsen K, Piana S, Dror RO, Eastwood MP, et al. Atomic-level characterization of the structural dynamics of proteins. Science 2010;330:341–6.
[19] Florian M. Coarse-graining in polymer simulation: from the atomistic to the mesoscopic scale and back. ChemPhysChem 2002;3:754–69.
[20] Nielsen SO, Lopez CF, Srinivas G, Klein ML. Coarse grain models and the computer simulation of soft materials. J Phys Condens Matter 2004;16:R481–512.
[21] Chakrabarty A, Cagin T. Coarse grain modeling of polyimide copolymers. Polymer 2010;51:2786–94.
[22] Zeng Q, Yu A, Lu G, Standish R. Molecular dynamics simulation of organic-inorganic nanocomposites: layering behavior and interlayer structure of organoclays. Chem Mater 2003;15:4732–8.
[23] Grest GS, Kremer K. Molecular dynamics simulation for polymers in the presence of a heat bath. Phys Rev A 1986;33:3628–31.
[24] Von Gottberg FK, Smith KA, Hatton TA. Stochastic dynamics simulation of surfactant self-assembly. J Chem Phys 1997;106:9850–7.
[25] Bourov GK, Bhattacharya A. The role of geometric constraints in amphiphilic self-assembly: a Brownian dynamics study. J Chem Phys 2003;119:9219–25.
[26] Öttinger HC. Brownian dynamics of rigid polymer chains with hydrodynamic interactions. Phys Rev E 1994;50:2696–701.
[27] Jain A, Sunthar P, Dünweg B, Prakash JR. Optimization of a Brownian-dynamics algorithm for semidilute polymer solutions. Phys Rev E 2012;85(066703):1–15.
[28] Hoogerbrugge P, Koelman J. Simulating microscopic hydrodynamic phenomena with dissipative particle dynamics. Europhys Lett 1992;19:155–60.
[29] Groot RD, Madden TJ, Tildesley DJ. On the role of hydrodynamic interactions in block copolymer microphase separation. J Chem Phys 1999;110:9739–49.
[30] Wijmans C, Smit B, Groot RD. Phase behavior of monomeric mixtures and polymer solutions with soft interaction potentials. J Chem Phys 2001;114:7644–54.
[31] Groot RD, Warren PB. Dissipative particle dynamics: bridging the gap between atomistic and mesoscopic simulation. J Chem Phys 1997;107:4423–35.
[32] Gibson JB, Chen K, Chynoweth S. Simulation of particle adsorption onto a polymer-coated surface using the dissipative particle dynamics method. J Colloid Interface Sci 1998;206:464–74.
[33] Dzwinel W, Yuen DA. A two-level, discrete particle approach for large-scale simulation of colloidal aggregates. Int J Mod Phys C 2000;11:1037–61.
[34] Baumgärtner A, Binder K, Hansen JP, Kalos M, Kehr K, Landau D, et al. Applications of the Monte Carlo method in statistical physics. New York: Springer Science & Business Media; 2013, 341 pp.
[35] Binder K. Monte Carlo and molecular dynamics simulations in polymer science. New York: Oxford University Press; 1995, 602 pp.
[36] Verdier PH, Stockmayer W. Monte Carlo calculations on the dynamics of polymers in dilute solution. J Chem Phys 1962;36:227–35.
[37] Rosenbluth MN, Rosenbluth AW. Monte Carlo calculation of the average extension of molecular chains. J Chem Phys 1955;23:356–9.
[38] Theodorou DN. Progress and outlook in Monte Carlo simulations. Ind Eng Chem Res 2010;49:3047–58.
[39] Vanderzande C. Lattice models of polymers. Cambridge: Cambridge University Press; 1998, 240 pp.
[40] Sadiq A. A new algorithm for the Monte Carlo simulation of spin-exchange kinetics of Ising systems. J Comput Phys 1984;55:387–96.
[41] Meng B, Weinberg W. Monte Carlo simulations of temperature programmed desorption spectra. J Chem Phys 1994;100:5280–9.
[42] Serebrinsky SA. Physical time scale in kinetic Monte Carlo simulations of continuous-time Markov chains. Phys Rev E 2011;83(037701):1–3.
[43] Aguado A, Madden PA. Ewald summation of electrostatic multipole interactions up to the quadrupolar level. J Chem Phys 2003;119:7471–83.
[44] Osychenko O, Astrakharchik G, Boronat J. Ewald method for polytropic potentials in arbitrary dimensionality. Mol Phys 2012;110:227–47.
[45] Wells BA, Chaffee AL. Ewald summation for molecular simulations. J Chem Theory Comput 2015;11:3684–95.
[46] Fredrickson GH, Ganesan V, Drolet F. Field-theoretic computer simulation methods for polymers and complex fluids. Macromolecules 2002;35:16–39.
[47] Fredrickson GH. The equilibrium theory of inhomogeneous polymers. Oxford: Oxford University Press; 2006, 452 pp.
[48] Edwards SF. The statistical mechanics of polymers with excluded volume. Proc Phys Soc 1965;85:613–24.
[49] Helfand E. Theory of inhomogeneous polymers: fundamentals of the Gaussian random-walk model. J Chem Phys 1975;62:999–1005.
[50] Helfand E. Block copolymer theory: III. Statistical mechanics of the microdomain structure. Macromolecules 1975;8:552–6.
[51] Matsen MW, Schick M. Stable and unstable phases of a diblock copolymer melt. Phys Rev Lett 1994;72:2660–3.
[52] Janert PK, Schick M. Phase behavior of ternary homopolymer/diblock blends: microphase unbinding in the symmetric system. Macromolecules 1997;30:3916–20.
[53] Helfand E, Wasserman Z. Block copolymer theory: 4. Narrow interphase approximation. Macromolecules 1976;9:879–88.
[54] Whitmore M, Vavasour J. Self-consistent mean field theory of the microphase diagram of block copolymer/neutral solvent blends. Macromolecules 1992;25:2041–5.
[55] Drolet F, Fredrickson GH. Combinatorial screening of complex block copolymer assembly with self-consistent field theory. Phys Rev Lett 1999;83:4317–20.
[56] Drolet F, Fredrickson GH. Optimizing chain bridging in complex block copolymers. Macromolecules 2001;34:5317–24.

[57] Fraaije J. Dynamic density functional theory for microphase separation kinetics of block copolymer melts. J Chem Phys 1993;99:9202–12.
[58] Fraaije J, Van Vlimmeren B, Maurits N, Postma M, Evers O, Hoffmann C, et al. The dynamic mean-field density functional method and its application to the mesoscopic dynamics of quenched block copolymer melts. J Chem Phys 1997;106:4260–9.
[59] Maurits N, Van Vlimmeren B, Fraaije J. Mesoscopic phase separation dynamics of compressible copolymer melts. Phys Rev E 1997;56:816–25.
[60] Knoll A, Lyakhova K, Horvat A, Krausch G, Sevink G, Zvelindovsky A, et al. Direct imaging and mesoscale modelling of phase transitions in a nanostructured fluid. Nat Mater 2004;3:886–91.
[61] Altevogt P, Evers O, Fraaije J, Maurits N, van Vlimmeren B. The MesoDyn project: software for mesoscale chemical engineering. J Mol Struct Theochem 1999;463:139–43.
[62] Maurits N, Fraaije J. Mesoscopic dynamics of copolymer melts: from density dynamics to external potential dynamics using nonlocal kinetic coupling. J Chem Phys 1997;107:5879–89.
[63] Sevink G, Charlaganov M, Fraaije J. Coarse-grained hybrid simulation of liposomes. Soft Matter 2013;9:2816–31.
[64] Sides SW, Kim BJ, Kramer EJ, Fredrickson GH. Hybrid particle-field simulations of polymer nanocomposites. Phys Rev Lett 2006;96(250601):1–4.
[65] Detcheverry FA, Kang H, Daoulas KC, Müller M, Nealey PF, de Pablo JJ. Monte Carlo simulations of a coarse grain model for block copolymers and nanocomposites. Macromolecules 2008;41:4989–5001.
[66] De Fabritiis G, Delgado-Buscalioni R, Coveney P. Multiscale modeling of liquids with molecular specificity. Phys Rev Lett 2006;97(134501):1–4.
[67] Kyrylyuk AV, Case FH, Fraaije J. Property prediction and hybrid modeling for combinatorial materials. QSAR Combin Sci 2005;24:131–7.
[68] Kang H, Detcheverry FA, Mangham AN, Stoykovich MP, Daoulas KC, Hamers RJ, et al. Hierarchical assembly of nanoparticle superstructures from block copolymer-nanoparticle composites. Phys Rev Lett 2008;100(148303):1–4.
[69] Kim JK, Yang SY, Lee Y, Kim Y. Functional nanomaterials based on block copolymer self-assembly. Prog Polym Sci 2010;35:1325–49.
[70] Lynd NA, Meuler AJ, Hillmyer MA. Polydispersity and block copolymer self-assembly. Prog Polym Sci 2008;33:875–93.
[71] Zhang L, Eisenberg A. Formation of crew-cut aggregates of various morphologies from amphiphilic block copolymers in solution. Polym Adv Technol 1998;9:677–99.
[72] Uneyama T, Doi M. Calculation of the micellar structure of polymer surfactant on the basis of the density functional theory. Macromolecules 2005;38:5817–25.
[73] Kawakatsu T. Computer simulation of self-assembling processes of a binary mixture containing a block copolymer. Phys Rev E 1994;50:2856–62.
[74] Ohta T, Ito A. Dynamics of phase separation in copolymer-homopolymer mixtures. Phys Rev E 1995;52:5250–60.
[75] Uneyama T, Doi M. Density functional theory for block copolymer melts and blends. Macromolecules 2005;38:196–205.
[76] Ohta T, Nonomura M. Elastic property of bilayer membrane in copolymer-homopolymer mixtures. Eur Phys J B 1998;2:57–68.
[77] Sun P, Yin Y, Li B, Chen T, Jin Q, Ding D, et al. Simulated annealing study of morphological transitions of diblock copolymers in solution. J Chem Phys 2005;122(204905):1–8.
[78] Shen H, Zhang L, Eisenberg A. Multiple pH-induced morphological changes in aggregates of polystyrene-block-poly(4-vinylpyridine) in DMF/H2O mixtures. J Am Chem Soc 1999;121:2728–40.
[79] Fredrickson GH, Sides SW. Theory of polydisperse inhomogeneous polymers. Macromolecules 2003;36:5415–23.
[80] Sides SW, Fredrickson GH. Continuous polydispersity in a self-consistent field theory for diblock copolymers. J Chem Phys 2004;121:4974–86.
[81] Jiang Y, Chen T, Ye F, Liang H, Shi AC. Effect of polydispersity on the formation of vesicles from amphiphilic diblock copolymers. Macromolecules 2005;38:6710–7.
[82] Terreau O, Luo L, Eisenberg A. Effect of poly(acrylic acid) block length distribution on polystyrene-b-poly(acrylic acid) aggregates in solution. 1. Vesicles. Langmuir 2003;19:5601–7.
[83] Jenekhe SA, Chen XL. Self-assembly of ordered microporous materials from rod-coil block copolymers. Science 1999;283:372–5.
[84] Cornelissen JJ, Fischer M, Sommerdijk NA, Nolte RJ. Helical superstructures from charged poly(styrene)-poly(isocyanodipeptide) block copolymers. Science 1998;280:1427–30.
[85] Chécot F, Lecommandoux S, Gnanou Y, Klok HA. Water-soluble stimuli-responsive vesicles from peptide-based diblock copolymers. Angew Chem Int Ed 2002;41:1339–43.
[86] Halperin A. Rod-coil copolymers: their aggregation behavior. Macromolecules 1990;23:2724–31.
[87] Lin J, Lin S, Zhang L, Nose T. Microphase separation of rod-coil diblock copolymer in solution. J Chem Phys 2009;130(094907):1–7.
[88] Lin S, Numasawa N, Nose T, Lin J. Brownian molecular dynamics simulation on self-assembly behavior of rod-coil diblock copolymers. Macromolecules 2007;40:1684–92.
[89] Ding W, Lin S, Lin J, Zhang L. Effect of chain conformational change on micelle structures: experimental studies and molecular dynamics simulations. J Phys Chem B 2008;112:776–83.
[90] Lin S, He X, Li Y, Lin J, Nose T. Brownian molecular dynamics simulation on self-assembly behavior of diblock copolymers: influence of chain conformation. J Phys Chem B 2009;113:13926–34.
[91] Lin Y, Chang H, Sheng Y, Tsao H. Structural and mechanical properties of polymersomes formed by rod-coil diblock copolymers. Soft Matter 2013;9:4802–14.
[92] Shah M, Ganesan V. Chain bridging in a model of semicrystalline multiblock copolymers. J Chem Phys 2009;130(054904):1–12.
[93] Song W, Tang P, Zhang H, Yang Y, Shi AC. New numerical implementation of self-consistent field theory for semiflexible polymers. Macromolecules 2009;42:6300–9.
[94] Ganesan V, Khounlavong L, Pryamitsyn V. Equilibrium characteristics of semiflexible polymer solutions near probe particles. Phys Rev E 2008;78(051804):1–10.
[95] Agrawal SK, Sanabria-DeLong N, Tew GN, Bhatia SR. Structural characterization of PLA-PEO-PLA solutions and hydrogels: crystalline vs amorphous PLA domains. Macromolecules 2008;41:1774–84.
[96] Cai C, Zhang L, Lin J, Wang L. Self-assembly behavior of pH-and thermosensitive amphiphilic triblock copolymers in solution: experimental studies and self-consistent field theory simulations. J Phys Chem B 2008;112:12666–73.
[97] He P, Li X, Kou D, Deng M, Liang H. Complex micelles from the self-assembly of amphiphilic triblock copolymers in selective solvents. J Chem Phys 2010;132(204905):1–6.
[98] Fromherz P. Lipid-vesicle structure: size control by edge-active agents. Chem Phys Lett 1983;94:259–66.
[99] Giacomelli FC, Riegel IC, Petzhold CL, da Silveira NP, Štěpaínek P. Aggregation behavior of a new series of ABA triblock copolymers bearing short outer A blocks in B-selective solvent: from free chains to bridged micelles. Langmuir 2008;25:731–8.
[100] Kong W, Li B, Jin Q, Ding D, Shi AC. Complex micelles from self-assembly of ABA triblock copolymers in B-selective solvents. Langmuir 2010;26:4226–32.
[101] He P, Li X, Deng M, Chen T, Liang H. Complex micelles from the self-assembly of coil-rod-coil amphiphilic triblock copolymers in selective solvents. Soft Matter 2010;6:1539–46.
[102] Li Y, Lin S, He X, Lin J, Jiang T. Self-assembly behavior of ABA coil-rod-coil triblock copolymers: a Brownian dynamics simulation approach. J Chem Phys 2011;135(014102):1–10.
[103] De Cuendias A, Ibarboure E, Lecommandoux S, Cloutet E, Cramail H. Synthesis and self-assembly in water of coil-rod-coil amphiphilic block copolymers with central π-conjugated sequence. J Polym Sci Part A Polym Chem 2008;46:4602–16.
[104] Lin CH, Tung YC, Ruokolainen J, Mezzenga R, Chen WC. Poly[2,;1; 7-(9, 9-dihexylfluorene)]-block-poly(2-vinylpyridine) rod-coil and coil-rod-coil block copolymers: synthesis, morphology and photophysical properties in methanol/THF mixed solvents. Macromolecules 2008;41:8759–69.
[105] Huang L, Hu J, Lang L, Zhuang X, Chen X, Wei Y, et al. “Sandglass”-shaped self-assembly of coil-rod-coil triblock copolymer containing rigid aniline-pentamer. Macromol Rapid Commun 2008;29:1242–7.
[106] Iatrou H, Frielinghaus H, Hanski S, Ferderigos N, Ruokolainen J, Ikkala O, et al. Architecturally induced multiresponsive vesicles from well-defined polypeptides: formation of gene vehicles. Biomacromolecules 2007;8:2173–81.
[107] Lin YL, Chang HY, Sheng YJ, Tsao HK. Self-assembled polymersomes formed by symmetric, asymmetric and side-chain-tethered coil-rod-coil triblock copolymers. Soft Matter 2014;10:1840–52.
[108] Gohy JF, Willet N, Varshney S, Zhang JX, Jérôme R. Core-shell-corona micelles with a responsive shell. Angew Chem Int Ed 2001;40:3214–6.
[109] Ma Z, Yu H, Jiang W. Bump-surface multicompartment micelles from a linear ABC triblock copolymer: a combination study by experiment and computer simulation. J Phys Chem B 2009;113:3333–8.
[110] Ma Z, Jiang W. Simulation study of aggregate morphologies formed by ABC linear triblock copolymers in a selective solvent through the self-consistent field theory. J Polym Sci Part B Polym Phys 2009;47:484–92.
[111] Wang R, Tang P, Qiu F, Yang Y. Aggregate morphologies of amphiphilic ABC triblock copolymer in dilute solution using self-consistent field theory. J Phys Chem B 2005;109:17120–7.
[112] Wang L, Lin J. Discovering multicore micelles: insights into the self-assembly of linear ABC terpolymers in midblock-selective solvents. Soft Matter 2011;7:3383–91.
[113] Jiang T, Wang L, Lin S, Lin J, Li Y. Structural evolution of multicompartment micelles self-assembled from linear ABC triblock copolymer in selective solvents. Langmuir 2011;27:6440–8.
[114] Chou SH, Tsao HK, Sheng YJ. Morphologies of multicompartment micelles formed by triblock copolymers. J Chem Phys 2006;125(194903):1–6.
[115] Zhao Y, Liu YT, Lu ZY, Sun CC. Effect of molecular architecture on the morphology diversity of the multicompartment micelles: a dissipative particle dynamics simulation study. Polymer 2008;49:4899–909.
[116] Li X, Pivkin IV, Liang H, Karniadakis GE. Shape transformations of membrane vesicles from amphiphilic triblock copolymers: a dissipative particle dynamics simulation study. Macromolecules 2009;42:3195–200.
[117] Li X, Liu Y, Wang L, Deng M, Liang H. Fusion and fission pathways of vesicles from amphiphilic triblock copolymers: a dissipative particle dynamics simulation study. Phys Chem Chem Phys 2009;11:4051–9.

[118] Zhou Y, Xia HG, Long XP, Xue XG, Qian W. Complex multicompartment micelles from simple ABC linear triblock copolymers in solution. Macromol Theory Simul 2015;24:85–8.
[119] Zhou C, Xia H, Zhou Y, Xue X, Luo S. Dissipative particle dynamics simulations of the morphologies and dynamics of linear ABC triblock copolymers in solutions. RSC Adv 2015;5:58024–31.
[120] Zhou Y, Long X, Xue X, Qian W, Zhang C. Morphologies and dynamics of linear ABC triblock copolymers with different block sequences. RSC Adv 2015;5:7661–4.
[121] Cui J, Jiang W. Vesicle formation and microphase behavior of amphiphilic ABC triblock copolymers in selective solvents: a Monte Carlo Study. Langmuir 2010;26:13672–6.
[122] Kong W, Jiang W, Zhu Y, Li B. Highly symmetric patchy multicompartment nanoparticles from the self-assembly of ABC linear terpolymers in C-selective solvents. Langmuir 2012;28:11714–24.
[123] Zhu Y, Yu H, Wang Y, Cui J, Kong W, Jiang W. Multicompartment micellar aggregates of linear ABC amphiphiles in solvents selective for the C block: a Monte Carlo simulation. Soft Matter 2012;8:4695–707.
[124] Breiner U, Krappe U, Jakob T, Abetz V, Stadler R. Spheres on spheres-a novel spherical multiphase morphology in polystyrene-*block*-polybutadiene-*block*-poly(methyl methacrylate) triblock copolymers. Polym Bull 1998;40:219–26.
[125] Liu S, Armes SP. The facile one-pot synthesis of shell cross-linked micelles in aqueous solution at high solids. J Am Chem Soc 2001;123:9910–1.
[126] Zhou Z, Li Z, Ren Y, Hillmyer MA, Lodge TP. Micellar shape change and internal segregation induced by chemical modification of a tryptych block copolymer surfactant. J Am Chem Soc 2003;125:10182–3.
[127] Kubowicz S, Baussard JF, Lutz JF, Thünemann AF, von Berlepsch H, Laschewsky A. Multicompartment micelles formed by self-assembly of linear ABC triblock copolymers in aqueous medium. Angew Chem Int Ed 2005;44:5262–5.
[128] Berlepsch H, Böttcher C, Skrabania K, Laschewsky A. Complex domain architecture of multicompartment micelles from a linear ABC triblock copolymer revealed by cryogenic electron tomography. Chem Commun 2009:2290–2.
[129] Schacher F, Walther A, Ruppel M, Drechsler M, Müller AH. Multicompartment core micelles of triblock terpolymers in organic media. Macromolecules 2009;42:3540–8.
[130] Uchman M, Stepanek M, Procházka K, Mountrichas G, Pispas S, Voets IK, et al. Multicompartment nanoparticles formed by a heparin-mimicking block terpolymer in aqueous solutions. Macromolecules 2009;42:5605–13.
[131] Stoenescu R, Meier W. Vesicles with asymmetric membranes from amphiphilic ABC triblock copolymers. Chem Commun 2002:3016–7.
[132] Luo L, Eisenberg A. One-step preparation of block copolymer vesicles with preferentially segregated acidic and basic corona chains. Angew Chem Int Ed 2002;41:1001–4.
[133] Liu F, Eisenberg A. Preparation and pH triggered inversion of vesicles from poly(acrylic acid)-*block*-polystyrene-*block*-poly(4-vinyl pyridine). J Am Chem Soc 2003;125:15059–64.
[134] Njikang G, Han D, Wang J, Liu G. ABC triblock copolymer micelle-like aggregates in selective solvents for A and C. Macromolecules 2008;41:9727–35.
[135] Helfrich W. Elastic properties of lipid bilayers: theory and possible experiments. Z Naturforsch C 1973;28:693–703.
[136] Markvoort A, Van Santen R, Hilbers P. Vesicle shapes from molecular dynamics simulations. J Phys Chem B 2006;110:22780–5.
[137] Wang L, Jiang T, Lin J. Self-assembly of graft copolymers in backbone-selective solvents: a route toward stable hierarchical vesicles. RSC Adv 2013;3:19481–91.
[138] Jain S, Bates FS. On the origins of morphological complexity in block copolymer surfactants. Science 2003;300:460–4.
[139] Jain S, Bates FS. Consequences of nonergodicity in aqueous binary PEO-PB micellar dispersions. Macromolecules 2004;37:1511–23.
[140] Cui H, Chen Z, Zhong S, Wooley KL, Pochan DJ. Block copolymer assembly via kinetic control. Science 2007;317:647–50.
[141] Wang X, Guerin G, Wang H, Wang Y, Manners I, Winnik MA. Cylindrical block copolymer micelles and co-micelles of controlled length and architecture. Science 2007;317:644–7.
[142] Hayward RC, Pochan DJ. Tailored assemblies of block copolymers in solution: it is all about the process. Macromolecules 2010;43:3577–84.
[143] Gradzielski M. Kinetics of morphological changes in surfactant systems. Curr Opin Colloid Interface Sci 2003;8:337–45.
[144] Narayanan T. High brilliance small-angle X-ray scattering applied to soft matter. Curr Opin Colloid Interface Sci 2009;14:409–15.
[145] Lund R, Willner L, Richter D. Kinetics of block copolymer micelles studied by small-angle scattering methods. In: Abex A, editor. Controlled polymerization and polymeric structures. Lee K-S: Berlin Heidelberg: Springer International Publishing; 2013. p. 51–158.
[146] Zhou Y, Yan D. Real-time membrane fusion of giant polymer vesicles. J Am Chem Soc 2005;127:10468–9.
[147] Savić R, Luo L, Eisenberg A, Maysinger D. Micellar nanocontainers distribute to defined cytoplasmic organelles. Science 2003;300:615–8.
[148] Noguchi H, Takasu M. Self-assembly of amphiphiles into vesicles: a Brownian dynamics simulation. Phys Rev E 2001;64(041913):1–7.
[149] Yamamoto S, Maruyama Y, Hyodo S. Dissipative particle dynamics study of spontaneous vesicle formation of amphiphilic molecules. J Chem Phys 2002;116:5842–9.
[150] Marrink SJ, Mark AE. Molecular dynamics simulation of the formation, structure, and dynamics of small phospholipid vesicles. J Am Chem Soc 2003;125:15233–42.
[151] He X, Schmid F. Dynamics of spontaneous vesicle formation in dilute solutions of amphiphilic diblock copolymers. Macromolecules 2006;39:2654–62.
[152] He X, Schmid F. Spontaneous formation of complex micelles from a homogeneous solution. Phys Rev Lett 2008;100(137802):1–4.
[153] Uneyama T. Density functional simulation of spontaneous formation of vesicle in block copolymer solutions. J Chem Phys 2007;126(114902):1–17.
[154] Huang J, Wang Y, Qian C. Simulation study on the formation of vesicle and influence of solvent. J Chem Phys 2009;131(234902):1–5.
[155] He X, Schmid F. Using prenucleation to control complex copolymeric vesicle formation in solution. Macromolecules 2006;39:8908–10.
[156] Harrison C, Adamson DH, Cheng Z, Sebastian JM, Sethuraman S, Huse DA, et al. Mechanisms of ordering in striped patterns. Science 2000;290:1558–60.
[157] Solis FJ, de la Cruz MO. Hydrodynamic coarsening of binary fluids. Phys Rev Lett 2000;84:3350–3.
[158] Zhang L, Sevink A, Schmid F. Hybrid lattice Boltzmann/dynamic self-consistent field simulations of microphase separation and vesicle formation in block copolymer systems. Macromolecules 2011;44:9434–47.
[159] Xu A, Gonnella G, Lamura A. Simulations of complex fluids by mixed lattice Boltzmann-finite difference methods. Phys A 2006;362:42–7.
[160] Tiribocchi A, Stella N, Gonnella G, Lamura A. Hybrid lattice Boltzmann model for binary fluid mixtures. Phys Rev E 2009;80(026701):1–7.
[161] Cates M, Henrich O, Marenduzzo D, Stratford K. Lattice Boltzmann simulations of liquid crystalline fluids: active gels and blue phases. Soft Matter 2009;5:3791–800.
[162] McCracken ME, Abraham J. Multiple-relaxation-time lattice-Boltzmann model for multiphase flow. Phys Rev E 2005;71(036701):1–9.
[163] Premnath KN, Abraham J. Three-dimensional multi-relaxation time (MRT) lattice-Boltzmann models for multiphase flow. J Comput Phys 2007;224:539–59.
[164] Mecke KR. Integral geometry in statistical physics. Int J Mod Phys B 1998;12:861–99.
[165] Chernomordik LV, Zimmerberg J, Kozlov MM. Membranes of the world unite! J Cell Biol 2006;175:201–7.
[166] Gröschel AH, Schacher FH, Schmalz H, Borisov OV, Zhulina EB, Walther A, et al. Precise hierarchical self-assembly of multicompartment micelles. Nat Commun 2012;3(710):1–10.
[167] Runge MB, Bowden NB. Synthesis of high molecular weight comb block copolymers and their assembly into ordered morphologies in the solid state. J Am Chem Soc 2007;129:10551–60.
[168] Košovan P, Kuldovaí J, Limpouchovaí Z, Prochaízka K, Zhulina EB, Borisov OV. Amphiphilic graft copolymers in selective solvents: molecular dynamics simulations and scaling theory. Macromolecules 2009;42:6748–60.
[169] Zhang L, Lin J, Lin S. Aggregate morphologies of amphiphilic graft copolymers in dilute solution studied by self-consistent field theory. J Phys Chem B 2007;111:9209–17.
[170] Qi H, Zhong C. Density functional theory studies on the microphase separation of amphiphilic comb copolymers in a selective solvent. J Phys Chem B 2008;112:10841–7.
[171] Chang HY, Lin YL, Sheng YJ, Tsao HK. Structural characteristics and fusion pathways of onion-like multilayered polymersome formed by amphiphilic comb-like graft copolymers. Macromolecules 2013;46:5644–56.
[172] Li M, Li GL, Zhang Z, Li J, Neoh KG, Kang ET. Self-assembly of pH-responsive and fluorescent comb-like amphiphilic copolymers in aqueous media. Polymer 2010;51:3377–86.
[173] Besseling N, Stuart MC. Self-consistent field theory for the nucleation of micelles. J Chem Phys 1999;110:5432–6.
[174] Kim KH, Huh J, Jo WH. Wirelike micelle formed by a T-shaped graft copolymer with a rigid backbone. Macromolecules 2004;37:676–9.
[175] Chen H, Ruckenstein E. Self-assembly of π-shaped copolymers. Soft Matter 2012;8:1327–33.
[176] Cai C, Lin J, Chen T, Tian X. Aggregation behavior of graft copolymer with rigid backbone. Langmuir 2010;26:2791–7.
[177] Hadjichristidis N, Pitsikalis M, Pispas S, Iatrou H. Polymers with complex architecture by living anionic polymerization. Chem Rev 2001;101:3747–92.
[178] Scholl M, Kadlecova Z, Klok HA. Dendritic and hyperbranched polyamides. Prog Polym Sci 2009;34:24–61.
[179] Wurm F, Frey H. Linear-dendritic block copolymers: the state of the art and exciting perspectives. Prog Polym Sci 2011;36:1–52.
[180] Sheiko SS, Sumerlin BS, Matyjaszewski K. Cylindrical molecular brushes: synthesis, characterization, and properties. Prog Polym Sci 2008;33:759–85.
[181] Choi YK, Bae YH, Kim SW. Star-shaped poly(ether-ester) block copolymers: synthesis, characterization, and their physical properties. Macromolecules 1998;31:8766–74.
[182] Liu H, Farrell S, Uhrich K. Drug release characteristics of unimolecular polymeric micelles. J Controll Release 2000;68:167–74.
[183] Havránková J, Limpouchová Z, Procházka K. Monte Carlo study of heteroarm star copolymers in good and selective solvents. Macromol Theory Simul 2003;12:512–23.

[184] Havránková J, Limpouchová Z, Procházka K. A new simulation algorithm with revised "association criteria" for studying the association of heteroarm star copolymers. Macromol Theory Simul 2005;14:560–8.
[185] Havránková J, Limpouchová Z, Štěpánek M, Procházka K. Self-assembly of heteroarm star copolymers-a Monte Carlo study. Macromol Theory Simul 2007;16:386–98.
[186] Yun J, Faust R, Szilágyi LS, Kéki S, Zsuga M. Effect of architecture on the micellar properties of amphiphilic block copolymers: comparison of AB linear diblock, A1A2B, and A2B heteroarm star block copolymers. Macromolecules 2003;36:1717–23.
[187] Han M, Hong M, Sim E. Influence of the block hydrophilicity of AB2 miktoarm star copolymers on cluster formation in solutions. J Chem Phys 2011;134(204901):1–9.
[188] Sheng YJ, Nung CH, Tsao HK. Morphologies of star-block copolymers in dilute solutions. J Phys Chem B 2006;110:21643–50.
[189] Li Z, Kesselman E, Talmon Y, Hillmyer MA, Lodge TP. Multicompartment micelles from ABC miktoarm stars in water. Science 2004;306:98–101.
[190] Xia J, Zhong C. Dissipative particle dynamics study of the formation of multicompartment micelles from ABC star triblock copolymers in water. Macromol Rapid Commun 2006;27:1110–4.
[191] Zhulina EB, Borisov O. Scaling theory of 3-miktoarm ABC copolymer micelles in selective solvent. Macromolecules 2008;41:5934–44.
[192] Kong W, Li B, Jin Q, Ding D, Shi AC. Helical vesicles, segmented semivesicles, and noncircular bilayer sheets from solution-state self-assembly of ABC miktoarm star terpolymers. J Am Chem Soc 2009;131:8503–12.
[193] Wang L, Xu R, Wang Z, He X. Kinetics of multicompartment micelle formation by self-assembly of ABC miktoarm star terpolymer in dilute solution. Soft Matter 2012;8:11462–70.
[194] Voit BI. Hyperbranched polymers-all problems solved after 15 years of research. J Polym Sci Part A Polym Chem 2005;43:2679–99.
[195] Voit BI, Lederer A. Hyperbranched and highly branched polymer architectures-synthetic strategies and major characterization aspects. Chem Rev 2009;109:5924–73.
[196] Peleshanko S, Tsukruk VV. The architectures and surface behavior of highly branched molecules. Prog Polym Sci 2008;33:523–80.
[197] Ballauff M, Likos CN. Dendrimers in solution: insight from theory and simulation. Angew Chem Int Ed 2004;43:2998–3020.
[198] Lescanec RL, Muthukumar M. Configurational characteristics and scaling behavior of starburst molecules: a computational study. Macromolecules 1990;23:2280–8.
[199] Radowski MR, Shukla A, von Berlepsch H, Böttcher C, Pickaert G, Rehage H, et al. Supramolecular aggregates of dendritic multishell architectures as universal nanocarriers. Angew Chem Int Ed 2007;46:1265–9.
[200] Wang Y, Li B, Zhou Y, Lu Z, Yan D. Dissipative particle dynamics simulation study on the mechanisms of self-assembly of large multimolecular micelles from amphiphilic dendritic multiarm copolymers. Soft Matter 2013;9:3293–304.
[201] Tan H, Wang W, Yu C, Zhou Y, Lu Z, Yan D. Dissipative particle dynamics simulation study on self-assembly of amphiphilic hyperbranched multiarm copolymers with different degrees of branching. Soft Matter 2015;11:8460–70.
[202] del Barrio J, Oriol L, Sánchez C, Serrano JL, Di Cicco A, Keller P, et al. Self-assembly of linear-dendritic diblock copolymers: from nanofibers to polymersomes. J Am Chem Soc 2010;132:3762–9.
[203] Wood KC, Little SR, Langer R, Hammond PT. A family of hierarchically self-assembling linear-dendritic hybrid polymers for highly efficient targeted gene delivery. Angew Chem Int Ed 2005;44:6704–8.
[204] Rosen BM, Wilson CJ, Wilson DA, Peterca M, Imam MR, Percec V. Dendron-mediated self-assembly, disassembly, and self-organization of complex systems. Chem Rev 2009;109:6275–540.
[205] Percec V, Wilson DA, Leowanawat P, Wilson CJ, Hughes AD, Kaucher MS, et al. Self-assembly of Janus dendrimers into uniform dendrimersomes and other complex architectures. Science 2010;328:1009–14.
[206] Lin YL, Chang HY, Sheng YJ, Tsao HK. Photoresponsive polymersomes formed by amphiphilic linear-dendritic block copolymers: generation-dependent aggregation behavior. Macromolecules 2012;45:7143–56.
[207] Mai Y, Zhou Y, Yan D. Real-time hierarchical self-assembly of large compound vesicles from an amphiphilic hyperbranched multiarm copolymer. Small 2007;3:1170–3.
[208] Ishizu K, Yamada H. Architecture of prototype copolymer brushes by grafting-from ATRP approach from functionalized alternating comb-shaped copolymers. Macromolecules 2007;40:3056–61.
[209] Verduzco R, Li X, Pesek SL, Stein GE. Structure, function, self-assembly, and applications of bottlebrush copolymers. Chem Soc Rev 2015;44:2405–20.
[210] Rzayev J. Molecular bottlebrushes: new opportunities in nanomaterials fabrication. ACS Macro Lett 2012;1:1146–9.
[211] Khalsa PS, Eisenberg SR. Compressive behavior of articular cartilage is not completely explained by proteoglycan osmotic pressure. J Biomech 1997;30:589–94.
[212] Seog J, Dean D, Plaas A, Wong-Palms S, Grodzinsky A, Ortiz C. Direct measurement of glycosaminoglycan intermolecular interactions via high-resolution force spectroscopy. Macromolecules 2002;35:5601–15.
[213] Hsu HP, Paul W, Binder K. One-and two-component bottle-brush polymers: simulations compared to theoretical predictions. Macromol Theory Simul 2007;16:660–89.
[214] Hsu HP, Paul W, Binder K. Structure of bottle-brush polymers in solution: a Monte Carlo test of models for the scattering function. J Chem Phys 2008;129(204904):1–11.
[215] Hsu HP, Paul W, Rathgeber S, Binder K. Characteristic length scales and radial monomer density profiles of molecular bottle-brushes: simulation and experiment. Macromolecules 2010;43:1592–601.
[216] Theodorakis P, Paul W, Binder K. Pearl-necklace structures of molecular brushes with rigid backbone under poor solvent conditions: a simulation study. J Chem Phys 2010;133(104901):1–9.
[217] Theodorakis PE, Paul W, Binder K. Interplay between chain collapse and microphase separation in bottle-brush polymers with two types of side chains. Macromolecules 2010;43:5137–48.
[218] Chang HY, Lin YL, Sheng YJ, Tsao HK. Multilayered polymersome formed by amphiphilic asymmetric macromolecular brushes. Macromolecules 2012;45:4778–89.
[219] Wang J, Guo K, An L, Müller M, Wang ZG. Micelles of coil-comb block copolymers in selective solvents: competition of length scales. Macromolecules 2010;43:2037–41.
[220] Lian X, Wu D, Song X, Zhao H. Synthesis and self-assembly of amphiphilic asymmetric macromolecular brushes. Macromolecules 2010;43:7434–45.
[221] Li Z, Hillmyer MA, Lodge TP. Control of structure in multicompartment micelles by blending μ-ABC star terpolymers with AB diblock copolymers. Macromolecules 2006;39:765–71.
[222] Voets IK, de Keizer A, de Waard P, Frederik PM, Bomans PH, Schmalz H, et al. Double-faced micelles from water-soluble polymers. Angew Chem Int Ed 2006;45:6673–6.
[223] Palyulin VV, Potemkin II. Mixed versus ordinary micelles in the dilute solution of AB and BC diblock copolymers. Macromolecules 2008;41:4459–63.
[224] Zhuang Y, Lin J, Wang L, Zhang L. Self-assembly behavior of AB/AC diblock copolymer mixtures in dilute solution. J Phys Chem B 2009;113:1906–13.
[225] Pispas S, Sarantopoulou E. Self-assembly in mixed aqueous solutions of amphiphilic block copolymers and vesicle-forming surfactant. Langmuir 2007;23:7484–90.
[226] Ma JW, Li X, Tang P, Yang Y. Self-assembly of amphiphilic ABC star triblock copolymers and their blends with AB diblock copolymers in solution: self-consistent field theory simulations. J Phys Chem B 2007;111:1552–8.
[227] Zhuang Z, Zhu X, Cai C, Lin J, Wang L. Self-assembly of a mixture system containing polypeptide graft and block copolymers: experimental studies and self-consistent field theory simulations. J Phys Chem B 2012;116:10125–34.
[228] Chen L, Jiang T, Lin J, åC Cai. Toroid formation through self-assembly of graft copolymer and homopolymer mixtures: experimental studies and dissipative particle dynamics simulations. Langmuir 2013;29:8417–26.
[229] Cai C, Li Y, Lin J, Wang L, Lin S, Wang XS, et al. Simulation-assisted self-assembly of multicomponent polymers into hierarchical assemblies with varied morphologies. Angew Chem Int Ed 2013;52:7732–6.
[230] Li Y, Jiang T, Lin S, Lin J, Cai C, Zhu X. Hierarchical nanostructures self-assembled from a mixture system containing rod-coil block copolymers and rigid homopolymers. Sci Rep 2015;5(10137):1–13.
[231] Balazs AC, Emrick T, Russell TP. Nanoparticle polymer composites: where two small worlds meet. Science 2006;314:1107–10.
[232] Hamley I. Nanotechnology with soft materials. Angew Chem Int Ed 2003;42:1692–712.
[233] Shenhar R, Norsten TB, Rotello VM. Polymer-mediated nanoparticle assembly: structural control and applications. Adv Mater 2005;17:657–69.
[234] Comotti M, Li WC, Spliethoff B, Schüth F. Support effect in high activity gold catalysts for CO oxidation. J Am Chem Soc 2006;128:917–24.
[235] Pan Q, Tong C, Zhu Y, Yang Q. Phase behaviors of bidisperse nanoparticle/block copolymer mixtures in dilute solutions. Polymer 2010;51:4571–9.
[236] Ma Z, Li RK. Effect of particle surface selectivity on composite nanostructures in nanoparticle/diblock copolymer mixture dilute solution. J Colloid Interface Sci 2011;363:241–9.
[237] Xu J, Han Y, Cui J, Jiang W. Size selective incorporation of gold nanoparticles in diblock copolymer vesicle wall. Langmuir 2013;29:10383–92.
[238] Cai C, Wang L, Lin J, Zhang X. Morphology transformation of hybrid micelles self-assembled from rod-coil block copolymer and nanoparticles. Langmuir 2012;28:4515–24.
[239] Thompson RB, Ginzburg VV, Matsen MW, Balazs AC. Predicting the mesophases of copolymer-nanoparticle composites. Science 2001;292:2469–72.
[240] Zhang L, Lin J, Lin S. Self-assembly behavior of amphiphilic block copolymer/nanoparticle mixture in dilute solution studied by self-consistent-field theory/density functional theory. Macromolecules 2007;40:5582–92.
[241] Li W, Zhang P, Dai M, He J, Babu T, Xu YL, et al. Ordering of gold nanorods in confined spaces by directed assembly. Macromolecules 2013;46:2241–8.
[242] Wang A, Huang J, Yan Y. Hierarchical molecular self-assemblies: construction and advantages. Soft Matter 2014;10:3362–73.
[243] Peterca M, Imam MR, Leowanawat P, Rosen BM, Wilson DA, Wilson CJ, et al. Self-assembly of hybrid dendrons into doubly segregated supramolecular polyhedral columns and vesicles. J Am Chem Soc 2010;132:11288–305.
[244] Lin SC, Ho RM, Chang CY, Hsu CS. Hierarchical superstructures with control of helicity from the self-assembly of chiral bent-core molecules. Chem Eur J 2012;18:9091–8.

[245] Wang W, Lin J, Cai C, Lin S. Optical properties of amphiphilic copolymer-based self-assemblies. Eur Polym J 2015;65:112–31.
[246] Xu H, Li Q, Wang L, He Y, Shi J, Tang B, et al. Nanoscale optical probes for cellular imaging. Chem Soc Rev 2014;43:2650–61.
[247] Jiang W, Kim BY, Rutka JT, Chan WC. Nanoparticle-mediated cellular response is size-dependent. Nat Nanotechnol 2008;3:145–50.
[248] Chen T, Guo X, Zhao A, Wang J, Shi C, Zhou S. Morphological transition of self-assembled architectures from PEG-based ether-anhydride terpolymers. Soft Matter 2013;9:3021–31.
[249] Chen T, Guo X, Liu X, Shi S, Wang J, Shi C, et al. A strategy in the design of micellar shape for cancer therapy. Adv Healthc Mater 2012;1:214–24.
[250] Alexander-Katz A, Moreira AG, Sides SW, Fredrickson GH. Field-theoretic simulations of polymer solutions: finite-size and discretization effects. J Chem Phys 2005;122(014904):1–8.
[251] Tang YH, Karniadakis GE. Accelerating dissipative particle dynamics simulations on GPUs: algorithms, numerics and applications. Comput Phys Commun 2014;185:2809–22.